5-2020

The Effects of Group II Metabotropic Glutamate Receptor Antagonism on Delayed Non-match to Odor Performance in Male Long-Evans Rats

Andrew Wolfarth
Montclair State University

Abstract

In recent years, there has been an increased interest in the role of glutamate, the brain's major excitatory neurotransmitter, in MDD. There is ample evidence that glutamate dysfunction is present in patients with varying degrees of depression. With this mechanistic shift behind MDD has come a better understanding of the importance of cognitive dysfunction in depressed patients. The general view of MDD was that it was a mood disorder, however recent evidence suggests that cognitive functioning is also critical to relief of depressive symptomology. Attempts have been made to modulate excitatory neural networks using a class of glutamate receptors known as ionotropic glutamate receptors (iGlu receptors). However, drugs which act on iGlu receptors lead to harmful exocitoxic effects and cognitive dysfunctions. Another subtype of glutamate receptor known as metabotropic glutamate receptors (mGlu receptors) may play a more modulatory role in excitatory neurotransmission. In the present study we investigated the role of the mGlu 2/3 receptor subtypes in cognitive function in Long Evans rats using a modified version of the delayed-nonmatch-to-sample task (DNMS). We made two hypotheses, 1) that the DNMS is a working memory task, in which accuracy decreases with increasing inter-trial intervals (ITI), 2) that antagonism of mGlu 2/3 receptors using LY341495 would improve working memory performance on the DNMS task. In congruence with our first hypothesis, performance on the DNMS task is decreased with increasing ITIs. However, LY341495 administration (30 min IP) impaired DNMS accuracy at 3 mg/kg and increased response latencies at 1 and 3 mg/kg. Therefore, it appears that increasing neuronal glutamate is not sufficient to improve cognitive functions such as working memory in normal subjects. Future studies may want to

investigate the effects of LY341495 using a biological model of depression like the chronic corticosterone model.

MONTCLAIR STATE UNIVERSITY

The Effects of Group II Metabotropic Glutamate Receptor Antagonism on Delayed Non-match to Odor Performance in Male Long-Evans Rats.

By

Andrew Wolfarth

A Master's Thesis Submitted to the Faculty of

Montclair State University

In Partial Fulfillment of the Requirements

For the Degree of

Master of Arts

May 2020

College of Humanities and Social Sciences

Department of Psychology

Thesis Committee:

[redacted]

Alan Pehrson
Thesis Sponsor

[redacted]

Adam Prus
Committee Member

[redacted]

Ruth Propper
Committee Member

The Effects of Group II Metabotropic Glutamate Receptor Antagonism on Delayed Non-Match to Odor Performance in Male Long-Evans Rats

A THESIS

Submitted in Partial Fulfillment of the Requirements for the Degree of Master of Arts

by

Andrew Wolfarth

Montclair State University

Montclair, NJ

2020

Table of Contents

List of Tables

List of Figures

Introduction

Depression, Economics, and Quality of Life Functioning

Major Depressive Disorder (MDD) is a common and severe mental disorder that impacts more than 264 million people and is currently the leading cause of global disability (WHO, 2017). MDD is associated with high rates of morbidity, nonremission and reoccurrence, and an economic burden amounting to nearly $210.5 billion per year (McIntyre et al., 2013; Muller et al., 1999; Porter, Gallagher, Thompson, & Young, 2003; National Institute of Mental Health, 2019; American Psychiatric Association Foundation, 2019).

Despite the large number of approved pharmacotherapies, current MDD treatments leave much to be desired. Nearly 1/3 of depressed patients find that current antidepressants are ineffective at treating their symptoms, and the majority of the current treatments take a significant amount of time to begin their effects (Hare & Duman., 2020). The general view of MDD has been that it is an affective mood disorder, with symptoms including lowered mood, loss of personal interests/relationships, and reduced quality of life (QOL) (McIntyre et al., 2013; Porter et al., 2003). But it is also a disorder of cognition. Recent reports suggest that MDD patients exhibit cognitive impairments in domains such as executive functioning (working memory and attention; Diamond, 2013), as well as psychomotor processing. Impaired patients often exhibit diminished decision making, concentrating, and reductions in self-care tasks (e.g. dressing, grooming). Patients with MDD generally exhibit measurable cognitive impairments that range from 1-2 standard deviations below the mean. Additionally, measures of effect sizes remain significant ranging from 0.2-0.6 in remitted MDD patients (McIntyre et al., 2013;

McIntyre et al., 2015a; Porter et al., 2003). Indeed, mood symptoms alone cannot account for the entire level of disability because cognitive impairments, and functional impairments associated with them, are still observed during mood symptom remission (Baune et al., 2010; Shimizu et al., 2013). MDD-related cognitive impairments are also associated with decreases in both motivation and the ability to sustain effort (Fava et al., 2014; Scheurich et al., 2008). Patients with MDD and healthy controls exhibit similar performance increases from motivational enhancements, but the MDD patients improve less and remain impaired on several cognitive functions. (Jazbec, McClure, Hardin, Pine, & Ernst, 2005; Richards & Ruff, 1989). Therefore, it appears that neither the severity of depression nor motivation levels can account for the level of cognitive impairment seen in MDD.

Understanding the role that cognitive dysfunction plays in MDD is important given recent studies suggesting that losses in functional ability is a major factor in MDD-associated economic costs (McIntyre et al., 2015; Rose & Ebmeier, 2006; Shimizu et al., 2013). While, there is little consensus what MDD features regulate QOL, mood symptoms do not appear to be a consistent predictor. Shimizu et al. (2013) reported that lower QOL levels are still present in patients with depressive-mood symptom remission. Additionally, where some studies found that depressive-mood symptom treatments can improve QOL, others found that it had little effect on QOL (Papakostas et al., 2004).

An alternative explanation for the persistence of QOL impairments may come from the relationship between MDD and cognitive dysfunction (Jaeger, Berns, Uzelac, & Davis-Conway, 2006). McCall & Dunn (2003) showed that poor self-evaluation scores on measures of daily living (IADL; instrumental appraisal of daily living) are associated

with reduced cognitive function in severely depressed patients. This idea is supported by findings from Jaeger et al. (2006) that cognitive dysfunction severity predicts functional recovery for patients with MDD. Further, McIntyre et al. (2015) demonstrated that cognitive dysfunctions remain significant predictors of global disability and workplace performance even when the depression severity was considered. Conversely, Baune et al. (2010) found that measures of QOL like the impairments of activities of daily living assessments (IADL/ADL) are not correlated with cognitive functioning. It is possible that these observed differences in the role of cognitive function in QOL can be explained by differences in age, disease state, and treatment methods of the participants. For example, the Kiosses and Alexopoulous (2005) found evidence for reduced IADL scores in geriatric patients with MDD, but Baune et al. (2010) did not in a sample with much wider age ranges. Thus, although there is still no clear consensus on the symptom clusters that drive reduced QOL scores in MDD patients, cognitive impairment may be a relevant mediating variable.

The Impact of Depression on Cognitive Functioning

According to Roiser and Sahakian (2013) cognitive functions can be divided into two domains consisting of hot and cold cognitive functions. Hot cognition includes functions tied to emotionally valanced stimuli such as anhedonia, negative biases in ruminative thoughts, recall and attention, and exaggerated reactions (McIntyre et al., 2015; Roiser & Sahakian, 2013). Cold cognition includes information processing functions that are not tied to emotional influences such as executive function, information processing speed, learning and memory, and attention/concentration (McIntyre et al., 2015; Roiser & Sahakian, 2013). It is common for patients with MDD to show impaired

performance across a range of cold cognitive functions such as memory (short-term and working memory), visuospatial processing, motor functioning, information processing speed, general intelligence and decision making (Roiser & Sahakian, 2013). Interestingly though, others have found this not to be the case, and have observed that patients with MDD do not perform significantly different than healthy controls (Barch et al., 2003). The inconsistency in these finding suggest that there may be issues with the methodology, heterogeneity of the samples, or the cognitive tasks. Many of the reported studies have failed to consider the issues of using mixed-groups, comorbid populations, age-related differences, or inclusion of subjects with multiple treatment methods (Matsuo et al., 2007; McIntyre et al., 2013). Thus, interpreting their collective meaning of these study outcomes is difficult. Additionally, even fewer studies have attempted to explore the nature of cognitive impairments prior to the onset of major depression (Marazziti, Consoli, Picchetti, Carlini & Faravelli, 2010), which may yield valuable data about how the disorder develops.

Overall, little attention has been paid to the effects of MDD on cognitive faculties such as short-term and working memory. Working memory is considered to be a form of short-term memory used to store and process complex information online for a limited duration (Baddeley, 2001; Barch, Sheline, Csernansky, & Synder 2003). Working memory is at best poorly understood and the literature does not suggest there is a consensus about it or its underlying components. There are generally only a few accepted measures of working memory for humans, and even fewer in the rodents. Further, many of the tests used to model depression in rodents can be understood to reflect either depressive-like behaviors or anxiety-related behaviors (Dudchenko, 2004). Additionally,

many of the measures used in both species report inconsistent results with varying interpretations. Many of the interpreted outcomes of these nonhuman tests make use of anthropomorphizations of depression without fully detailing the biological substrates underlying the observations (Chiriţă, Gheorman, Bondari, Rogoveanu, 2015; Pu et al., 2011). These issues can create issues when trying to use these models to develop successful treatments in humans.

History of Tasks Used to Model Depression in Humans and Rodents

When drawing comparisons between rodent and animal models, it is important to remember that there are structural differences in the rodent PFC and that of non-human primates and humans. In rodents, the medial prefrontal cortex (mPFC) is considered to be the equivocal structure to the dorsolateral prefrontal cortex in humans (Liu et al., 2014). The rodent mPFC is generally understood to include the prelimbic (PL) and infralimbic (IL), as well as the anterior cingulate cortex (ACC). The ventral portion of the mPFC corresponds to the subgenual cortex (Brodmann area 25) while the more dorsal mPFC is related to the ACC in human and non-human primates. In animal models, working memory tasks typically make use of temporal delays or variations of spatial cues, without regard to capacity, a subtopic that is beyond the scope of this investigation. Clinical evidence suggests that for rodent models of memory function, non-matching-to sample tasks (NMS) are a valid method to assess working memory impairments (Davies, Molder, Greba, & Howland, 2013; Dudchenko, 2004; Dudchenko, Wood, & Eichenbaum, 2000). The NMS tasks as described by Dudchenko (2004) are a two trial (information/retention) task that requires the subject to differentiate between a set of old and new stimuli in order to receive a reward. A useful aspect of the NMS task is that it can be modified to remove

spatial cues and to introduce temporal delays (delayed-nonmatch-to-sample, DNMS), which allows the researcher to modify task difficulty or memory load.

The DNMS task requires the subject to remember a stimulus over a delay period and to be able to correctly identify and select a novel stimulus from the previously presented one when presented with both simultaneously. While it is possible to evaluate working memory using other tasks such as the spontaneous exploration task. Measures like the DNMS task are inversely correlated with increases in the temporal delay period, a common hallmark of working memory function. DNMS tasks also give researchers the advantage of specifying what content is to-be-remembered during the task rather than having to interpret what the animal remembered. Stern et al., (2001) suggests that during the DNMS task, repeated presentations of small numbers of stimuli can result in significantly slower learning and reduced performance in nonhuman primates. Additionally, the literature suggests that rats trained on DMNS tasks which use repeated stimuli are not able to learn the task as easily as a DNMS with unique stimuli (Dudchenko, 2004; Wood et al., 1999). Such evidence may indicate that there is a fundamental difference in the memory systems used to encode familiar vs unique stimuli. The repeated use of a small set of familiar stimuli requires the subject to maintain the information about the stimuli leading to the possibility of interference effects (Schon et al., 2008). Whereas unique stimuli do not produce the same interference effects and have been shown to be more reliant on recognition memory and hippocampally dependent (Mumby, 2001). It is likely that the PFC is responsible for maintaining active representations of stimuli during the DNMS in order to avoid interference effects (Dudchenko, 2004; Stern et al., 2001), another feature commonly associated with

working memory functioning. Davies et al. (2013,2017) have shown that in rats, the mPFC is needed to maintain performance on working memory span tasks. An idea that is supported by lesion studies showing that damage to the PFC results in stronger impairments on the DNMS with 8 but not 16 odors (Stern et al., 2001). Therefore, a DNMS task which makes use of a small number of repeated stimuli may represent more ethologically valid measure of the PFC involvement of working memory.

Models of the Pathophysiology of Depression in Humans

Despite the high prevalence rates and clear socioeconomic burden, there is little agreement on the pathophysiological mechanisms behind major depressive disorder. Studies indicate that cognitive impairments seen in MDD are the result of neurobiological abnormalities, which have been observed using structural and functional neuroimaging techniques (Barch et al., 2003; Matsuo et al., 2007; Pu et al., 2011). However, it should be noted that these studies also suffer from inconsistent results showing differences in activation patterns or in structure/functional form. Patients with MDD have physiological and hemodynamic changes in areas like the hippocampus, amygdala, caudate nucleus, putamen and prefrontal cortex (PFC) (Chiriţă et al., 2015; Matsuo et al., 2007; Pu et al., 2011). Additionally, studies report reductions in glial cell counts, and deceased neuronal size and/or synaptic proteins within these regions (Rajkowska et al., 1999). Using positron emission tomography, it has been found that depressed patients display significant reductions in PFC volume which appears to be correlated with the duration of the disorder. The evidence suggests that this reduction in volume is not necessarily due to neuronal loss, as the literature often suggests, but rather in reductions of synapses which is evidenced by reduced ligand binding (Hare & Duman., 2020). Such changes in the

structure/function of the PFC are also observed animal studies which show that chronic stress models of depression can reduce the density of dendritic spines in areas like the mPFC.

The PFC has been implicated in the functioning of personality, awareness, and cognition including working memory, and MDD-related mood symptoms. Investigations into the physiology behind depression using populations with treatment resistant depression have shed light on the importance of the PFC in depressive symptomology. Application of deep brain stimulation within areas like the subgenual cingulate (Brodmann area 25) markedly improves mood with some capacity to improve cognitive functioning (Mayberg et al., 2005; McNeely et al., 2008). Interestingly, the improvement in mood and cognitive functioning observed by McNeely and colleagues (2008) was not statistically correlated. Lending further support to the idea the cognitive dysfunction is a separate domain of depression distinct from mood symptoms. Damage to the PFC results in significant deficits in tasks designed to measure working memory (Bechara, Damasio, Tranel, & Anderson, 1998; Müller & Knight, 2006). More specifically, the dorsolateral prefrontal cortex in human and nonhuman primates has been shown to be involved with working memory (Granon, Vidal, Thinus-Blanc, Changeux, & Poucet, 1994). In human patients with MDD, scores on working memory test such as the n-back are significantly lower compared to healthy controls (Matsuo et al., 2007). Matsuo et al., (2007) showed that healthy individuals had bilateral activation of the DLPFC, left inferior frontal gyrus, and anterior cingulate (ACC) during the n-back task compared to patients with MDD which had greater activation (hyperactivation) in the left PFC and cingulate cortex during working memory tasks. fMRI studies have supported the role of

the PFC's ability to maintain consistent responses to repeated presentations of stimuli. The PFC is preferentially engaged when prior representations already exist in the brain and must be selectively updated and monitored to avoid interference(Stern, Sherman, Kirchhoff, & Hasselmo, 2001). Such evidence suggests that activity within the cortico-limbic circuit may serve an important role in working memory function (Matsuo et al., 2007). Conversely, Barch et al., (2003) observed that there are no differences in PFC activation on the n-back task between MDD patients and healthy controls using fMRI. Others have also suggested that there is hypoactivation rather than hyperactivation in the PFC of MDD patients (Pu et al., 2011). Therefore, it should be clear that the association between frontal activation and task performance is not always consistent and there must be a more complex explanation underlying these differences.

The Pharmacological Characteristics of Metabotropic Glutamate Receptors 2 and 3

Within the prefrontal cortex glutamate is the primary excitatory neurotransmitter. Glutamate receptors can be divided into two types based on their method of activation and so are referred to as either ionotropic glutamate receptors (iGlu receptors) or metabotropic glutamate receptors (mGlu receptors). iGlu receptors contain specialized ion channels that have selective affinities for *N*-methyl-*D*-aspartate (NMDA), α-amino-3-hydroxy-5-methyl-4-isoxazolepropionic acid (AMPA), and kainate.

The mGlu receptor class can be divided into three subgroups and eight distinct subtypes. Metabotropic glutamate receptors are grouped together based on sequence homology, intracellular second messengers, ligand selectivity and pharmacological properties. Group II (mGlu receptor 2 and mGlu receptor 3) mGlu receptors share roughly 67% sequence homology and are coupled to Gi/o G-protein alpha subunits

(Cartmell & Schoepp, 2002; Chaki, Ago, Palucha-Paniewiera, & Pilc, 2013; Gu et al., 2008a; Ottersen & Landsend, 1997; G. Richards et al., 2005). mGlu 2/3 receptors binding to Gi/o negatively regulates intracellular cAMP levels, leading to inhibition of voltage-gated calcium channels. Interestingly, a majority of the studies that have investigated the effects of group II mGlu receptor effects on calcium channel inhibition have done so using mGlu 2/3 receptor agonists while observing postsynaptic activity in areas like the neocortex, hippocampus (CA1 and CA3), and the striatum. The evidence suggests that this inhibition occurs most commonly in N-type calcium channels but also in L-type and P/Q type channels. N-type calcium channel inhibition can occur relatively fast by Group II selective agonists in a way that appears to be the result of a direct membrane delimiting action involving the G-protein rather than a diffusible intracellular second messenger. Inhibition of these N-type calcium channels appears to be related to the slowing of activation kinetics within isolated neocortical neurons as well as human embryo kidney cells (HEK) that express both mGlu 2/3 receptors. Whereas the blocking of L-type inhibition can be generated by external Ca^{2+} in neocortical pyramidal cells and appears to occur in a relatively slow manner, which fits that characteristics of a diffusible intracellular second messenger. Little work has been done of the effects of P/Q calcium channel inhibition, but the data suggests that they can be blocked by (1R)-1-aminocyclopentane-1,3-dicarboxylic acid (t-ACPD), (1R,2R)-3-[(S)-amino(carboxy)methyl]cyclopropane-1,2-dicarboxylic acid (DCG-IV) and quisqualate in the frontal and parietal cortices. Additionally, G-protein βγ subunits may directly stimulate inhibitory G protein inwardly rectifying potassium channels (GIRKs). mGlu receptors 2/3 functional coexpression on GIRK subunits has led to the finding that group

II mGlu receptor agonist can activate inhibitory GIRK-mediated currents (Anwyl, 1999; Dutar et al., 1999, 2000; Knoflach & Kemp., 1998).

In either case, activation of mGlu 2/3 receptors induces modulatory inhibitory effects on cellular activation which may make them good candidates for drug targets. Compared to iGlu receptors, group II mGlu receptors may have to potential to act as drug targets for depression and anxiety treatments. The activation of iGlu receptors often lead to excitotoxic effects, and inhibition can have serious health side effects (Wierońska & Pilc, 2009). Evidence suggests group II mGlu receptors can be expressed either pre-or-postsynaptically(Gu et al., 2008b; Neki et al., 1996). Presynaptic mGlu 2/3 receptors could decrease neurotransmitter release via voltage-gated calcium channel inhibition. Postsynaptically expressed mGlu 2/3 receptors can potentially stimulate GIRKS or alter cAMP regulation to reduce cellular depolarizations (Anwyl, 1999; Iacovelli, Nicoletti, & De Blasi, 2013; Johnson & Schoepp, 2008; Suh, Kai, & Roche, 2018). A result of sharing such a close sequence makes understanding how the mGlu 2/3 receptors are distributed, and their functional properties a challenge to the field.

Among the mGlu receptor ligands exists agonists such as (1S,2S,5R,6S)-2-aminobicyclo[3.1.0]hexane-2,6-dicarboxylic acid (LY354740), (1S,2R,5R,6R)-2-amino-4-oxabicyclo[3.1.0]hexane-2,6-dicarboxylic acid (LY379268), (2R,4R)-4-aminopyrrolidine-2,4-dicarboxylic acid (LY314593), DCG-IV, (1S,2S)-2-[(1S)-1-amino-2-hydroxy-2-oxoethyl]cyclopropane-1-carboxylic acid (L-CCG-I), and (4S,6S)-4-amino-2-thiabicyclo[3.1.0]hexane-4,6-dicarboxylic acid (LY389795) which the literature suggests are selective for group II mGlu 2/3 receptors. There are also mGlu 2/3 receptor selective antagonists like (2S)-2-Amino-2-[(1S,2S)-2-carboxycycloprop-1-yl]-3-(xanth-9-

yl)propanoic acid (LY341495), (1S,2S)-2-[(2S)-2-amino-1-hydroxy-1-oxopropan-2-yl]cyclopropane-1-carboxylic acid (MCCG), (1R,2R,3R,5R,6R)-2-amino-3-[(3,4-dichlorophenyl)methoxy]-6-fluorobicyclo[3.1.0]hexane-2,6-dicarboxylic acid (MGS0039) (Johnson & Schoepp, 2008). Most of the known mGlu 2/3 receptor ligands cross-react, and only a few can discriminate between the two receptor types which has important implications when considering their distributions and functional roles. For more details about the affinities of LY341495 and LY354740 for mGlu receptors see *Table 1*. Antagonism of mGlu 2/3 receptors is thought to possess antidepressant like effects in tasks like the force swim test, tail suspension test, and the learned helplessness test in rodents (Bespalov et al., 2008; Wierońska & Pilc, 2009).

Regional Distribution of Metabotropic Glutamate Receptors 2 and 3

There have been several attempts to map the distribution of Group II mGlu receptors, using techniques such as autoradiography, immunohistochemistry, and *in situ* hybridization, but not all report consistent results. Investigations into the distribution of mGlu 2/3 receptors based on mRNA expression and immunoreactivity suggest they are localized on neurons and glia in areas associated with higher cognitive functions (Prefrontal Cortex, Hippocampus, Amygdala, Basal Ganglia) and areas involved in sensory perceptions (Olfactory bulb, Somatosensory Cortex, Thalamus: Cartmell & Schoepp, 2002; Feyissa et al., 2010; Ohishi, Shigemoto, Nakanishi, & Mizuno, 1993a, 1993b; Tanabe et al., 1993, Marek, 2010). Immunostaining using an antibody which identified both mGlu 2 receptors and mGlu 3 receptors indicated that mGlu 2/3 receptors are moderately expressed on neurons and in the neuropil of the cerebral cortex.

Throughout the rodent neocortex, immunostaining of mGlu 2/3 receptors was light to moderate with higher levels observed in layers I, III and IV compared to layers II, V, VI. Staining on neurons was largely observed on small/medium neurons in many of the layers, with scattered staining seen on pyramidal neurons in layers III and V. The pattern of immunoreactivity in the neocortex appears to correspond well with distribution mGlu 2/3 receptor mRNA transcripts (Petralia et al., 1996; Richards & Ruff, 1989). In the hippocampus, mGlu 2/3 receptors immunostaining was light to moderately observed in areas CA1-CA3. In areas CA1-CA3 mGlu 2/3 receptor immunoreactivity was commonly found on the neuropil and irregular processes located between pyramidal neurons. There was little evidence for labeling on neuronal cell bodies, but some labeling was observed on pyramidal neurons in areas CA1. Additionally, in areas CA1-CA3 light to moderate staining was seen on glial cell bodies and processes assumed to be astroglia. In areas of the hippocampal formation like the dentate gyrus, moderate levels of immunolabeling was seen on granular and molecular layers. Immunolabeling extended into the layers of the entorhinal cortex and was largely seen in the neuropil with only few neurons expressing immunoreactivity. Overall, the pattern of immunoreactivity observed in the hippocampal formation corresponds well with the distribution of mRNA seen by Richards et al., (2005). Immunoreactivity in the basal ganglia was seen largely in the neuropil in a light to moderate manner with densest staining in striatum. Within the striatum, immunoreactivity was dense and seen throughout whole of the structure. The observed immunoreactive cells were largely neuropil with only scattered expression on neurons and dendrites. Interestingly, mGlu 2 mRNA appeared to be absent in the striatum

but mGlu 3 mRNA could be clearly seen throughout the structure (Petralia et al., 1996; Richards & Ruff, 1989).

In humans, mGlu 3 mRNA was localized on neurons in the cerebral cortex, and highly expressed within the white matter. Expression within the dentate gyrus was similar to that seen in rodent granular layers(Harrison et al., 2008).While the studies of human mRNA expression of group II mGlu receptors can differentiate between mGlu 2 and mGlu 3 receptors, majority of the studies that have used mGlu 2/3 immunoreactive antibodies cannot. Harrison et al. (2008) indicates that immunolabeling is present within white matter, and on structures like the striatum, hippocampus, and PFC with strongest expression in the neocortex. In the frontal cortices labeling was not expressed on neurons, dendrites, or glial cell bodies, and exhibited a pre-perisynaptic localization. Within the hippocampus, mGlu 2/3 receptor immunoreactivity is present throughout the structure (CA1-CA4 and dentate gyrus), and localized on granular and pyramidal neurons, glia, and neuropil.

Cellular and Subcellular Distribution of Metabotropic Glutamate Receptor 2

On a subcellular level, mGlu 2 receptors are expressed predominantly on neurons with some evidence suggesting they are also found on glia (Ohishi et al., 1993a; Ghose et al., 2008). The localization of the mGlu 2 receptor appears to favor pre- and peri-synaptic zones that are situated away from the synaptic site of activity, with some evidence for post-synaptic expression (Anwyl, 1999; Cartmell & Schoepp, 2002; Neki et al., 1996; Petralia et al., 1996; Richards et al., 2005). In the neocortex, mGlu 2 mRNA was weak to moderately observed in all layers I-VI. mRNA expression was most dense in layer IV and least dense in layers I and VI. mRNA transcripts were present on pyramidal and non-

pyramidal neurons in all layers except layer I (Gu et al., 2008b; Ohishi et al., 1993a). Observations of mGlu 2 receptor immunoreactive cells show a similar pattern of distribution compared to mGlu 2 mRNA transcripts. Some differences within the layers indicate a stronger localization in layers II-V (Gu et al., 2008b). In the hippocampus mGlu 2 receptor mRNA labeling was irregularly distributed in areas CA1-CA3, and widely expressed in the granular layer of the dentate gyrus (Ohishi et al., 1993a). The levels of immunoreactivity in hippocampal areas CA1-CA3 matched the mRNA expression in these areas, as well as within the granular layer of dentate gyrus (Ohishi et al., 1993a). Gu et al., (2007) also reported intense immunolabeling from the dentate mossy fibers extending into the hippocampal area CA3. While much of the immunoreactivity in the hippocampal formation match the mRNA expression, Gu et al., (2007) observed different levels of immunoreactivity in the dentate gyrus. The level of intensity seen by Gu and colleagues (2007) indicated that mGlu 2 labeling throughout the dentate was only low to moderate, with the observed intensity on individual granular cells appearing to be only moderately intense. Such differences may be explained by the ability for the antibody to identify mGlu 2 proteins. In the striatum there was only a light level of mGlu 2 mRNA expression observed throughout the entire structure with mGlu 2 receptors mRNA being weakly expressed on neurons (Gu et al., 2008b; Ohishi et al., 1993a). Immunoreactivity in the striatum confirms the weak and sporadic distribution of mGlu 2 mRNA (Gu et al., 2008a). Additional evidence suggests that mGlu 2 receptors can function as heterodimers with other receptors such as mGlu3, mGlu 4, and serotonergic $5HT_{2A}$ receptors (Doumazane et al., 2011; J. Liu et al., 2017; Schoepp, 2001). Based on the localization and electrophysiological evidence, mGlu 2 receptors

may play a role as presynaptic autoreceptors that inhibit the release of glutamate and possibly other neurotransmitters under high frequency stimulation (Chaki et al., 2013; Iacovelli et al., 2013; Lovinger & McCool, 1995; Schoepp, 2001).

Cellular and Subcellular Distribution of Metabotropic Glutamate Receptor 3

Research into distribution pattern of the mGlu 3 receptor mRNA and immunoreactivity indicates they are expressed predominantly on neurons and glia. Evidence suggests that the mGlu 3 receptor is localized on the periphery and away from the postsynaptic site of action (Anwyl, 1999; Cartmell & Schoepp, 2002; Ohishi et al., 1993b; Petralia et al., 1996; G. Richards et al., 2005). However, because of the poor ability for group II mGlu receptor ligands to discriminate between mGlu 2 receptors and mGlu 3 receptors, distribution and localization patterns suggested by the literature may not be accurate. Using mGlu 2 receptor knockout mice and a mGlu 3 receptor specific antibody indicates that presynaptic mGlu 3 receptors are localized away from the synaptic zone of activity, whereas postsynaptic mGlu 3 receptors are localized closer to synapse (Johnson & Schoepp, 2008; Tamaru et al., 2001). The mGlu 3 receptor appears to have less neuronal expression and higher glial expression compared to the mGlu 2 receptor but is distributed in many of the same regions (Ohishi et al., 1993b). In the cerebral neocortex of mice, mGlu 3 receptors immunoreactivity was found diffusely in all layers, with strongest expression in layers I-III, weaker in IV-VI, and diffusely throughout the neuropil. In the cingulate cortex, mGlu 3 receptor immunostaining was diffusely distributed in a pattern similar to the neocortex (I-III > IV-VI). Within the hippocampus, mGlu 3 receptor immunoreactivity in area CA1 was weakly expressed in the neuropil of the stratum lacunmosum moleculare, and moderate in the strata radiatum

and oriens. In area CA3 stratum lacunmosum moleculare, intense staining was seen in the neuropil, with moderate expression in the strata radiatum and oriens. Additionally, mGlu 3 receptor immunolabeling was intense in the neuropil of dentate gyrus molecular layer and the striatum (McOmish et al., 2016; Tamaru et al., 2001).

Interestingly these immunostaining results in mice agree with the mRNA localization of the mGlu 3 receptor in rats, but not with the intensity of the distribution which may indicate a cross species difference in mGlu 3 receptor expression. In the cerebral cortex mGlu 3 receptor mRNA was distributed on pyramidal and non-pyramidal neurons, as well as glia cells such as astrocytes and oligodendrocytes. mGlu 3 receptor mRNA has a moderate level of expression in neocortical layers IV-VI and is only weakly labeled in layers I-III (Ohishi et al., 1993). mRNA staining was observed on both pyramidal and nonpyramidal neurons in a weak to moderate level in these layers. However, the expression of mGlu 3 mRNA does not appear to be consistent, Gu et al., (2007) observed a difference in the expression levels seen within the neocortex of rats compared to Ohishi and colleagues (1993). Gu et al., (2007) saw mGlu 3 receptor mRNA levels within the neocortex as being light to moderate, with lowest layer I having the least and layer IV having the highest expression. In layers II, III, V, and VI mGlu 3 receptor mRNA expression was considered light to moderate. Within the hippocampal formation, weak to no mRNA staining observed in the stratum lacunmosum moleculare (CA1 only), the stratum radiatum, pyramidal cell and granule cell layers of CA1 and CA3. In the hippocampal granular layer, mGlu 3 receptor mRNA labeled cells were irregularly distributed on neurons and glia. mRNA labeling was seen throughout dentate gyrus was intense, but only lightly expressed on individual granular cells. In the striatum and

nucleus accumbens many neurons were weak to moderately labeled (Gu et al., 2008b; Harrison et al., 2008; Johnson & Schoepp, 2008; Ohishi et al., 1993). Like the mGlu 2 receptors, the mGlu 3 receptors may form heterodimers and regulate the release of glutamate and other neurotransmitters (Chaki et al., 2013; Johnson & Schoepp, 2008).

Role of Metabotropic Glutamate Receptors 2/3 and Glia in the Tripartite Synapse

The classical model of neurotransmission generally involves what is called a bipartite synapse consisting of a pre-synaptic terminal and post-synaptic density. Such bidirectional signaling has been observed in both neuron-neuron but also neuron-glia transmission. A common type of neuron-glia transmission occurs with metabotropic glutamate receptors and astrocytes (Wierońska & Pilc, 2009). Such interactions between glia and neurons has led to the proposal of a three-way interacting synapse called the tripartite synapse (*Figure 1*). The tripartite synapse is composed of three interactive compartments: a presynaptic and postsynaptic terminal, and an astrocyte. Astrocytes are known to receive inputs, process information and send signals to other cells, all without being able to fire action potentials or conduct electrical excitability. Functionally, astrocytes play a role in neuroprotection and plasticity, suggesting they may be involved with a variety of neurocognitive disease pathologies. A common hallmark of depression pathology is the reduction in glia-to-neuron ratio (Sanacora et al., 2012). Astrocytic loss could explain the dysregulation in glutamatergic signaling observed in depressed patients. Interestingly, astrocytes possess g-protein coupled receptor sites for many neurotransmitters, such as mGlu 3 receptors. In areas like the cerebral cortex, mGlu 3 receptors have higher expression rates on glial processes compared to synaptic terminals. Such glial processes are also commonly found around other neurotransmitter terminals

such as GABA (Wierońska & Pilc, 2009). For a model of the distribution of mGlu 2/3 receptors at the tripartite synapse see *Figure 1*.

Once activated, mGlu receptors localized on astrocytes can regulate excitatory synaptic transmission by controlling the levels of extracellular glutamate through the release of gliotransmitters. Such activation is generally associated with increased uptake or removal of glutamate from the synaptic cleft which would decrease excitatory signaling. Therefore, antagonism of astrocytic mGlu 3 receptors could increase levels of synaptic glutamate and excitatory signaling. (Wierońska & Pilc, 2009).

Hypothesized Role of Metabotropic Glutamate Receptors 2 and 3 in Rat

The importance of glutamate neurotransmission can be seen in its relationship to cognitive functions like learning and memory. Glutamatergic synapses play a role in both long-term potentiation (LTP) and long-term depression (LTD), both of which are important factors for the integration of new information (Sanacora et al., 2012). The existing literature indicates that decreases in excitatory activity within the frontal cortex either impairs or improves cognitive function. The group II mGlu 2/3 receptor subtypes are widely expressed in brain regions important for short-term and working memory (frontal cortex/ mPFC) (Johnson & Schoepp, 2008; Ohishi et al., 1993a,1993b). Localization studies suggest mGlu 2/3 receptors are expressed pre-post-synaptically and in the periphery away from the synaptic zone of activity. Activation of presynaptic mGlu 2/3 receptors regulates the release of and prevents excessive buildup of glutamate. In addition, activation of postsynaptic mGlu 2/3 receptors can negatively modulate neuronal excitability through intracellular mechanisms. mGlu 2/3 receptors agonists reduce activity of the host cell through inhibition of calcium channels or activation of GIRKS

(Johnson & Schoepp, 2001). Antagonization of the mGlu 2/3 receptors should lead to an increase in glutamate neurotransmission through a combination of neuronal and glial mechanisms. This ability to modulate excitatory activity is worth investigation given the abundance of glutamatergic pyramidal cells within the frontal cortex compared to inhibitory GABAergic cells, as well as the ability for mGlu 2/3 receptors to form heterodimers and to regulate the release of other neurotransmitter receptors (GABA, Dopamine, 5-HT2A) (Chaki et al., 2013; Johnson & Schoepp, 2008).

It has been previously hypothesized that increasing glutamate neurotransmission should improve cognitive function (Gregory et al., 2003; Pehrson et al., 2016). In congruence with this, it has been proposed that using the mGlu 2/3 receptor antagonist LY341495 to increase glutamate levels in would facilitate cognitive performance on short-term working memory tasks (Gregory et al., 2003; Higgins et al., 2004). Given that the DNMS is considered to be a working memory task, we hypothesize here that increasing the temporal delays between information and retention trials will decrease overall task accuracy. Additionally, we hypothesize that increasing levels of neuronal glutamate in the rat brain via the group II mGlu receptor antagonist LY341495 would facilitate performance during the odor based delayed-non-match-to-sample task.

Methods

Subjects

Twenty-two Male Long Evans male rats (*age 6-8 weeks, Envigo*) were tested using a within-subjects design. After arriving to the facility, the rats were paired housed, and placed in a room with a 12hr light/dark cycle (8:00AM to 8:00PM). For one week, the rats had ad libitum access to food and water. Otherwise, the rats had ad libitium

access to water and were placed on a diet to maintain them at 90% of their free feeding weight. Experiments were approved by and conducted in accordance with the Montclair State University Institutional Animal Care and Use Committee and were consistent with the *Guide for the Care and Use of Laboratory Animals (2010)*.

Apparatus

An open field platform designed according to the specifications of Davies et al. (2004) (*91cm L x 91cm W x 91cm H*) with a (*5 cm)* surrounding wall was used throughout the training and testing procedures (see Figure 2). The platform was fastened to a pole which sat *91* cm off the floor. The platform was placed inside of an arrangement of four black welders' currents to block out any external visual cues. To secure the Nalgene cups (*2.5cm D x 2.9cm H*) to the open field, they were attached to Velcro strips that were evenly spaced 14 cm apart, and 8cm in from the wall.

Drugs

(2S)-2-Amino-2-[(1S,2S)-2-carboxycycloprop-1-yl]-3-(xanth-9-yl) propionic acid (LY341495) disodium salt was purchased from Tocris Bioscience (Minneapolis, MN). LY341495 was dissolved in sterile saline and pH was adjusted to 7.2-7.8. Vehicle or LY341495 was administered intraperitoneally (I.P.) 30 minutes prior to the start of behavioral testing. LY341495 was administered at final doses of 0.3, 1, or 3 mg/kg. Doses represent the mass of the active base, not the salt. All injections were administered at a volume of 1 mL/kg of body weight.

Odors

The odor cues were a mixture of sand (Sakrete; Atlanta, Georgia) and spices (see Table 2) that were placed inside of the Nalgene cups. The sand mixtures consisted of

(99.5 grams) sand and (0.5 grams) a single dry spice with a powered consistency (any dry leaf spices were ground to a powder using a mortar and pestle). Initially, the experiment started with 12 scents. However, because of suspected difficulty differentiating between two scents (e.g. cumin seed, and basil), those two were replaced with two different scents (e.g. lemon peel, and thyme). In total 14 scents were used throughout the duration of the experiment. All the spices were store-bought, and brand remained consistent when replenished. The odors and odor sequences used for a particular day were selected using Random.org's random list generator. For a single testing day all rats experienced the same odors but the order at which the odors were presented were randomized for each individual.

Habituation

Rats were handled individually for five minutes once a day for one week prior to training. After the week of handling, each rat individually experienced a single five-minute habituation session to acclimate them to environment of the open field.

Shaping Training

Following the habituation training, the rats were trained how to dig for a food reward (Fruit Loops, Kellogg's, Battle Creek, Michigan) that was buried in unscented sand. The shaping training consisted of three consecutive phases. In phase one, the rats were allowed to explore the open field with a single cup of unscented sand with the food reward placed on top of the sand and in the middle of the cup. Once the rat consumed the reward they were removed from the open field. During all of the phases and between each rat, the field was cleaned with a Virkon cleaning solution (Lanxess, Cologne, Germany). Phase two consisted of the same unscented sand cup but with the food reward

partially buried in the sand. The third phase again used the same unscented sand cup, but the food reward was fully buried (3 mm deep) in the sand. Throughout phases one and two, the rats had an unlimited amount of time to explore and retrieve the reward. Exploration time for phase three was reduced to 5minutes. After experiencing all three phases within a single day, training consisted of a single phase three testing session where the rat had five minutes to explore and retrieve the food.

Group II had a time limit of 5 minutes established for all three phases of the training and experienced all three phases daily. In total, shaping training spanned a total of 5 to 25 days, depending on the performance of individual animals.

When a rat was consistently failing to meet the time criteria and was considered to as having difficulty understanding the task. Standard shaping training as standard above was replaced with an incremental digging training which consisted of the following. These incremental sessions included six trials in which the food reward got buried deeper until it was buried 3mm deep by the final trial. The passing criteria for the shaping training required the rats to be able to retrieve the food reward within thirty seconds for three consecutive testing days. Of the twenty-two rats that experienced the shaping training, twenty-one successfully completed the training within an average of 13 sessions, see *Figure 7A*.

Non-matching-to-Sample Task

Once the rats met passing criteria for shaping training, they began training on the non-matching-to-sample task (NMS). This experiment utilized a modified version of the NMS as described in (Davies et al., 2013). The modification that was incorporated into this study required the location of the stimulus cups to be fully randomized in both the

information and retention trial. All locations were randomly generated using a random sequence generator and then pseudo-randomly assigned to avoid instances with repeated locations between trials. During the information trial, the rats had to retrieve a fully buried food reward from a single cup of scented sand mixture. Once the rats consumed the food reward they were removed and placed in their home cage. For the retention trial, the rats were presented with both the original scented sand mixture without the reward, and a cup containing different novel scented sand with a fully buried reward. The rat's choice was scored as correct if they removed the reward from the novel scented cup without touching the original cup from the information trial. For both the information and retention trials, the rats had a maximum of 30 seconds to retrieve the reward, which was the minimum speed at which the trials could be setup. The training criterion for NMS training required the rats to score a minimum of 5:6 correct trials for three consecutive testing days. If the rats experienced difficulty in learning the task, they were given incremental digging training across all six sessions until they could reliably retrieve the reward. The NMS training the Group I and Group II rats experienced were methodologically identical. Of the twenty-one rats that began the NMS training, 14 completed the training (mean 16 sessions).

Delayed Non-matching to Sample Task

Once the rats were able to reliable pass the NMS and successfully completed the supplementary experiments, they moved onto the delayed non-match-to sample task (DNMS). The setup and procedure for the DNMS was the same as the NMS but used an intertrial time interval (ITI) between the information and retention trials that was established from the results of the supplementary experiment 1. The ITI used in the

DNMS was 100 seconds which was judged as being an ITI that could have room for improved task accuracy.

Experimental Design

Supplementary Experiment 1: Assessing the Effects of Time on Memory Performance

The NMS task as a measure of working memory should be expected to have decreased performance as the time interval between information and retention trials gets longer. To investigate this aspect of the NMS task, all rats that met NMS passing criteria were assigned four different intertrial time intervals (30, 100, 300, and 1000 seconds) using a Randomized Latin square design.

Supplementary Experiment 2: Assessing the Use of Alternate Task Completion Strategies

All rats (n=14) that met NMS criteria were given two probes that investigated whether the rats were marking the cups during the trials, or if they were using the scent of the food reward as a guide. The reward probe proceeded the same as the regular NMS task, but the food reward was removed from the novel cup during the retention trial. If the novel cup was selected, the food reward was placed on top of the sand. To rule out the possibility that the rats were marking the cups. The odor probe replaced the original cup present during the information trial with a new cup containing the same scent as the original. If the rats failed to meet NMS criteria during either probe trial, they were removed from the NMS training before beginning drug trials.

Primary Experiment: The Effects of LY341495 DNMS Task Performance

The rats that proceeded onto the DNMS LY341495 trials (n=11) had previously completed the NMS training, the NMS ITI, and the NMS supplementary probes. The

LY341495 DNMS task was methodologically identical to the DNMS task stated above. It consisted of six sessions (12 trials) with a 100 second ITI between the information and retention trials. LY341495 dosing during the DNMS used a within-subjects design, and the order of dosing (vehicle, 0.3, 1, 3 mg/kg) was determined using a randomized Latin square design. LY341495 doses were all administered via intraperitoneal (I.P) injections 30 minutes prior to the start of the initial information trial. For a single testing day, each rat received a single dose, and were exposed to one testing session consisting of six trials. Between each dosing day the rats were retested on the regular DNMS task to ensure they could still perform the task. During the LY341495 trials 3 rats failed to reach the DNMS criteria and were removed from the LY341495 trials. A total of 8 rats completed the LY341495 trials.

Data Analysis

The primary dependent measure was defined *a priori* as an accuracy measurement, expressed as a percentage of the total number of trials within a given test session in which a correct choice was made during a given test session for an individual animal. Secondary dependent measures included latency to choose a digging pot, and the distance traveled during the information and retention trials (collected by SMART video tracking software, Harvard Apparatus, Holliston, MA).

Inferential statistical analysis for all dependent measures was conducted using the same analysis plan, which was defined *a priori*. First, data was checked for normality using the Lilliefors test. In cases where data was distributed normally, data was analyzed using a one-way repeated measures ANOVA, with Tukey-Kramer post hoc tests where appropriate. In cases where data was not distributed normally, data was analyzed using

Friedman's test, followed where appropriate by the Wilcoxon-Ranked Sign post hoc tests. All data are expressed as mean ± standard error of the mean (SEM), and alpha was set at 0.05.

Results

Probe Trial Data

Raw data for probe trials are presented in Table 3. There was a total of 14 rats that were tested on the probe trials, all data are presented in *Figure 5.* The passing criteria was set the same as the DNMS ≥ 83.3% accuracy. During the reward probe all 14 rats passed with 100% accuracy, indicating that the rats were not guided by the scent of the reward. Inspection of the accuracy data during the marking probe revealed that three rats were guided by some form of marking odor, achieving less than < 83.3% accuracy. The three rats which failed the marking probe were removed from the study leaving 11 rats to proceed onto the LY341495 DNMS trials.

A description of sample sizes after each stage of training, probe trials, or testing can be found in Figure 3.

Time Course Data

Raw data for ITI trials is presented in Table 4. To validate the DNMS as a working memory task the effects of the inter-trial-interval (ITI) on the accuracy data are presented in *Figure 6*. Investigation of the ITI accuracy data using the Lilliefors's test of normality indicates that the data was not normally distributed ($D_n = 0.15625$, $p < 0.05$), therefore the non-parametric Friedman's test was used for inferential analysis. The results of the Friedman's test on the accuracy data during the ITIs suggests that the data is

significantly different compared to the accuracy at the ITI of ($\chi^2(3) = 16.4$, $p < 0.05$). We used Kendall's W to measure effect size for the Friedman's test, and found a value of 0.681, which is interpreted as a moderate effect size and indicates the data points are in moderate agreement with each other. Post hoc analysis with the Wilcoxon signed-rank test revealed there was a significant difference between the 30 seconds and 100 seconds ($Z = -3.09$, $p < 0.05$), 30 seconds and 300 seconds ($Z = -3.42$, $p < 0.05$), and 30 seconds and 1000 seconds ($Z= -3.39$, $p < 0.05$).

LY341495 Effects on the DNMS Task

During the course of the LY341495 DNMS task three rats were removed because of failure to achieve passing criteria on follow-up testing. All data from the LY341495 DNMS task (n=8) are as follows.

The Effects of LY341495 on DNMS Task Accuracy

Raw data for LY341495 DNMS trials is presented in Table 5. The effects of LY341495 on accuracy data are presented in *Figure 7*. Investigation of the accuracy data using the Lilliefors's test of normality indicates that the data was not normally distributed ($D_n = 0.18975$, $p < 0.05$), therefore the non-parametric Friedman's test was used for inferential analysis. The results of the Friedman's test suggest that LY341495 dose had a significant effect on accuracy ($\chi^2(3) = 9.6$, $p < 0.05$). We used Kendall's W to measure effect size for the Friedman's test, and found a value of 0.398, which is interpreted as a moderate effect size and indicates the data points are in moderate agreement with each other. Post hoc analysis with the Wilcoxon signed-rank test revealed there was no differences between the vehicle and 0.3 mg/kg doses ($Z = -1.51$, n.s.) or the vehicle and 1

mg/kg doses (Z = -0.412, n.s.). However, there was a statistically significant decrease between the vehicle and 3 mg/kg doses (Z = -2.48, $p < 0.05$).

The Effects of LY341495 on DNMS Distance Traveled

Raw data for LY341495 DNMS trials is presented in Table 5. The effects of LY341495 on distance traveled data are presented in *Figure 8.* The assumption of normality was checked using the Lilliefors's test which showed that the data was normally distributed ($D_n = 0.1205$, n.s.), therefore we could proceed with the inferential analysis using a one-way repeated measures ANOVA. The results of the ANOVA indicated there was a statistically significant difference between the groups for the distance traveled data as determined by the one-way repeated measures ANOVA ($F(3,27) = 4.588$, $p = .0127$). This analysis was associated with an η^2 of 0.284, which indicates the data had a moderately large effect size. We used a post hoc analysis using the Tukey's HSD method showed there was no statistically significant difference between the distances traveled at any of the doses (0.3, 1 and 3 mg/kg) compared to vehicle.

The Effects of LY341495 on DNMS Latency to Retrieve the Reward

Raw data for LY341495 DNMS trials is presented in Table 5. The effects of LY341495 on latency to retrieve the reward data are presented in *Figure 8.* We used the Lilliefors's test to check the assumption of normality, which indicated that the data was not normally distributed ($D_n = 0.25915$, $p < 0.05$), therefore the non-parametric Friedman's test for inferential statistics is appropriate. Analysis of the latency data using the Friedman's test indicated that LY341495 had a significant effect on response latency ($\chi^2(3) = 11.8$, $p = 0.00792$); W= 0.494). We used Kendall's W to measure effect size for the Friedman's test, and found a value of 0.494, which is interpreted as a moderate effect

size and indicates the data points are in moderate agreement with each other. Post hoc analysis using the Wilcoxon signed-rank test revealed that there were no detectable differences between the vehicle and the 0.3 mg/kg dose (Z= -1.73, n.s). However, there was a statistically significant increase in latency between the vehicle dose and the 1 mg/kg (Z = -2.58, $p < 0.5$), as well as the vehicle dose and the 3 mg/kg (Z= -2.26, $p < 0.5$).

The Effects of LY341495 on DNMS Locomotor Speed

Raw data for LY341495 DNMS trials is presented in Table 5. The effects of LY341495 on locomotor speed data are presented in *Figure 8.* Using the Lilliefors's test of normality revealed that the latency data was normally distributed ($D_n = 0.13914$, $p > 0.05$), therefore we can proceed with a one-way repeated measures ANOVA. Results of the one-way repeated measures ANOVA on the locomotor speed traveled at indicates that there were no statistically significant differences between the groups ($F(3,27) = 1.026$, n.s, $\eta^2 = 0.232$). Using the generalized eta-squared as a measure of effect size found a value of ($\eta^2 = 0.232$), which indicates the data had a large effect size.

Discussion

We hypothesized that by increasing the temporal delays (ITI) between the DNMS information and retention trials there would be an overall decrease in task accuracy. Analysis of the ITI data indicates that this hypothesis was correct, and that task accuracy dropped with increasing ITIs. Additionally, it was hypothesized that increasing the levels of neuronal glutamate in the rat brain via the group 2 mGlu receptor antagonist LY341495 would facilitate working memory performance during the DNMS task. Our data suggests that administration of LY341495 during the DNMS impairs delayed non-

match to sample performance in a dose-dependent manner, becoming statistically significant at 3 mg/kg. The analysis of the distance the rats traveled during the task indicated a significant main effect of treatment but did not differ between the dosing groups. Furthermore, LY34195 treatment increased latency for the rats to remove the food reward at 1 and 3 mg/kg doses. Finally, LY341495 did not alter locomotor speed exhibited by the rats during the DNMS. There was no analysis done on measures such as thigmotaxia. These data indicate that LY341495 administration impaired memory function with limited effects on motor function.

The takeaway from the ITI data gives support to the idea that the DNMS task is a working memory task. Increasing the ITI markedly reduced performance in the task. Given that LY341495 is selective for group II mGlu receptors but unable to differentiate between receptors in that class, and that each has a similar but unique distribution within the CNS complicates our findings. Interpretations of the cognitive effects of LY341495 on DMNS accuracy indicate that increases in glutamate functioning may have a level at which it can improve cognitive performance during the DNMS task. Support for this comes from the accuracy data which indicates that while a 1 mg/kg dose was not significantly different than vehicle, accuracy scores at this dose were higher compared to 0.3 and 3 mg/kg. Alternatively, it may suggest that the model of improving cognitive functioning through increasing glutamate is too simplistic. The underlying mechanisms controlling glutamate and its role in the CNS may be more complex than the current literature suggests, a topic discussed further below.

The Effects of mGlu 2/3 Agonism and Antagonism on Cognitive Function

When drawing comparisons about the effects of LY341495 on non-spatial working memory functioning it is important to note that there are relatively few studies that have explored this niche. With that, our results are somewhat consistent with the literature of LY341495's effect on cognitive functioning. Gregory and colleagues (2003) showed that microinjections of the antagonist LY341495 directly into the PFC of rats produces a trend towards increased performance during the forced choice delayed-alternation task on a T-maze, a task often considered to model working memory performance. Using the novel object recognition (NOR) test in rats, Pitsikas et al., (2012) showed that LY341495 administered intraperitoneally at the same doses also impaired the ability to perform the task. Interestingly, and most likely due to the differences in neuronal systems activated during the NOR and DNMS, the observed decreases in the NOR task performance were in the opposite direction as the DNMS (higher doses = less impairment). Additionally, in mice LY341495 at both 1 and 3 mg/kg has been shown to attenuate impairments in cognitive function during the delayed non-match to position task produced by LY354740 (Higgins et al., 2004). Conversely, Gregory et al., (2003) was showed that microinjections of LY341495 produced a trend towards increased working memory performance on the forced choice delayed-alternation task using a T-maze.

The results of LY341495 on measures of locomotion in the present study differ somewhat from the literature. In the NOR task used by Pitsikas et al., (2012), LY34495 did not produce any off-target effects such as changes in locomotion, whereas it did in

our DNMS task. However, in mice, administration of LY34195 significantly increased the locomotor activity in a dose-dependent manner (Bespalov et al., 2007).

Interestingly, the literature suggests that antagonism and agonism of mGlu 2/3 receptors can produce similar effects on cognition. A common and selective drug used to activate group 2 mGlu receptors is LY354740. Several studies using LY354740 indicate that agonism of mGlu 2/3 receptors can impair working memory functions on a variety of tasks and across species (Aultman & Moghaddam, 2001; Spinelli et al., 2005). However, LY354740 can also attenuate working memory impairments produced by disruptions in glutamatergic transmission (Aultman & Moghaddam, 2001; Krystal et al., 2005). Application of LY354740 and LY341495 produces a competitive effect of mGlu 2/3 receptors. In some cases, LY341495 can attenuate the impairments produced by LY354740 (Higgins et al., 2004).

The Role of mGluRs in Long-term Depression and Long-term Potentiation of Synaptic Transmission

The reported inhibitory actions of mGlu 2/3 receptors in the CNS suggests that they may play a significant role in the long-term depression of synaptic transmission, a form a plasticity highly involved with learning and memory (Collingridge et al., 2010; Vose & Stanton, 2016). The induction of LTD by mGlu 2/3 receptors is a phenomenon observed it a variety of species such as humans, non-human primates, and rodents. Additionally, LTD has been implicated in pathology of cognitive dysfunctions commonly seen in depression. Within the mPFC mGlu 2/3 activation of receptors located in proximity to layer V pyramidal cells (more specifically mGlu 3 receptors) have been observed to suppress electrically-evoked excitatory postsynaptic potentials (EPSP) (Barbara et al.,

2003; Xie & Steketee, 2009). Postsynaptic mGlu 2/3 induced LTD in areas like the PFC through a variety of systems. In the PFC, LTD can be regulated through activation of PKC and PKA pathways which can be regulated by postsynaptic group II mGlu receptors (Otani et al., 2002). Whereas, in the hippocampal areas CA1 and CA3 there is contradiction about the role of mGlu 2/3 receptor induced LTD. By using mGlu 2 receptor knockout mice Yokoi and colleagues (1996) were able to show that mGlu 2 receptors are needed to induce LTD at the CA3 mossy fibers. However, pharmacological evidence suggests that tonic activation of mGlu 2/3 receptors is not sufficient to induce LTD within hippocampal areas CA1 and CA3 (Kemp & Bashir, 1999; Wostrack & Dietrich, 2009). Group II mGlu receptor mediated LTD has also been observed in areas like amygdala, striatum, nucleus accumbens, and in the cerebellum (Kahn et al., 2001). In the striatum, Kahn and colleagues (2001) were able to show that activation of mGlu 2/3 receptors was sufficient to induce LTD corticostriatal synapses. Within the amygdala, LTD can be mediated by activation of mGlu 2/3 receptors in rat, or solely by mGlu 3 receptors in mGlu 2 receptor knockout mice (Lucas et al., 2013). Additionally, in the nucleus accumbens presynaptic group 2 mGlu receptors mediate LTD through inhibition of Ca^{2+} channels (Robbe et al., 2002).

In addition to the role of mGlu 2/3 receptors in the induction of LTD, mGlu 2/3 receptors are also involved in the regulation of long-term potentiation (LTP). LTP is known as the long-term enhancement of synaptic transmission. mGlu 2/3 receptor mediated enhancements of synaptic transmission have been observed in area of the hippocampal formation such as areas CA1 and the dentate gyrus but the evidence is not always consistent. In the dentate gyrus, application of group II agonist LY354740

mediates LTP and can be attenuated with LY341495 (Wu et al., 2004). However, Kilbride and colleagues (1998) showed that when LY35470 is applied to the medial performant path of the dentate gyrus mGlu 2/3 receptors (most likely presynaptically located) decrease EPSPs and induce LTD. To further the contradictory role of mGlu 2/3 receptors in LTP and LTD, application of LY341495 in rats on high fat diets known to impair cognition, can stimulate LTP in the dentate gyrus (Karimi et al., 2015). Within the hippocampal area CA1, agonism of mGlu 2/3 receptors induces LTP whereas antagonism blocks LTP. Interestingly, the observed LTP in CA1 may be mediated through mGlu 2/3 receptors located on glial cells, given the low levels of presynaptic neuronal mGlu 2/3 receptors (Grover et al., 1999). In congruence with Grover et al. (1999), Behnisch and colleagues (1998) observed that activation of mGlu 2/3 receptors reduced LTP, however antagonization of these receptors appears to facilitate LTP in CA1 of the hippocampus.

Limitations and Conclusions

In the present study there were some methodological considerations that should be discussed. During drug trials, vehicle treated animals exhibited high levels of performance despite the fact that there was an ITI of 100 seconds. This indicates that order effects are important, and the animal's performance at the task improved during training. Such evidence may indicate that the DNMS is partially dependent on other brain regions besides the PFC. Alternatively, it could be that the present ceiling effects are a result of the inability to improve cognitive functioning in nonimpaired animals. Future studies could use a model of depression such as the chronic corticosterone model. It has been observed that LY341495 administered via i.p injections (0.1 & 0.3 mg/kg; 10ml/kg

body weight) reduces immobility time during the forced swim test in chronic corticosterone treated mice (Ago et al., 2012).

There is also possibility that our sample size could influence the results of the statistical analysis. While it is not uncommon for rodent studies to use small samples, such as in (Davies et al., 2013; Pitsikas et al., 2012; Waterhouse et al., 2003), small sample sizes can lead to increased rates of false positives in the results. Such considerations cannot be avoided in our study given that statistical test like the one-way repeated measures ANOVA on the LY341495 distance data was significant, but post-hoc Tukey's test could not detect significant group differences. It would be ideal for future studies to repeat our methods using a larger sample to size to validate the results we obtained.

Additionally, LY341495 is generally considered to be a group II mGlu receptor selective antagonist but the literature does suggest that it also has affinity for group 1 (mGlu 5) and group 3 (mGlu 8) mGlu receptors (Johnson et al., 1999). Taking this into account warrants that idea that effects of LY341495 in the present study may not have been fully mGlu 2/3 receptor dependent. For more details about the affinities of LY341495 and LY354740 for mGlu receptors see *Table 1*. In addition, because we did not directly measure the levels of neuronal glutamate after administration of LY341495 and given that LY341495 decreases EPSP in the PFC, the hypothesis proposed here may have misinterpreted the mechanistic role of mGlu 2/3 receptor antagonism in cognitive functioning. Alternatively, the observed impairment produced by LY341495 may be due to the use systemic administration rather than local. Given the wide distribution of mGlu 2/3 receptors, especially in areas related to olfactory sensing (Spooren et al., 2003),

LY341495 may have affected glutamatergic neurotransmission in other regions needed to perform that task successfully.

In conclusion, the mGlu 2/3 antagonist LY341495 impairs working memory function in a dose-dependent manner in the odor-based DNMS task. Additionally, LY341495 produced effects on the locomotor behavior of rats. However, LY341495 administered at 1 mg/kg produced less functional impairment than a lower dose at 0.3 mg/kg and a higher dose at 3 mg/kg. Future studies may want to further investigate the role of mGlu 2/3 receptor antagonism using more selective drugs and attempt to replicate these findings.

References

Ago, Y., Yano, K., Araki, R., Hiramatsu, N., Kita, Y., Kawasaki, T., ... & Baba, A. (2013). Metabotropic glutamate 2/3 receptor antagonists improve behavioral and prefrontal dopaminergic alterations in the chronic corticosterone-induced depression model in

American Psychiatric Association Foundation. (n.d.). Quantifying the Cost of Depression. Retrieved from http://www.workplacementalhealth.org/Mental-Health Topics/Depression/Quantifying-the-Cost-of-Depression.

Anwyl, R. (1999). Metabotropic glutamate receptors: electrophysiological properties and role in plasticity. Brain research reviews, 29(1), 83-120.

APA: Haahr, M. (2020). RANDOM.ORG: True Random Number Service. Retrieved from https://www.random.org

Armstrong JF, Faccenda E, Harding SD, Pawson AJ, Southan C, Sharman JL, Campo B, Cavanagh DR, Alexander SPH, Davenport AP, Spedding M, Davies JA; NC-IUPHAR. (2019) The IUPHAR/BPS Guide to PHARMACOLOGY in 2020: extending immunopharmacology content and introducing the IUPHAR/MMV Guide to MALARIA PHARMACOLOGY. Nucl. Acids Res. pii: gkz951. doi: 10.1093/nar/gkz951

Aultman, J. M., & Moghaddam, B. (2001). Distinct contributions of glutamate and dopamine receptors to temporal aspects of rodent working memory using a clinically relevant task. Psychopharmacology, 153(3), 353-364.

Barbara, J. G., Auclair, N., Roisin, M. P., Otani, S., Valjent, E., Caboche, J., ... & Crepel, F. (2003). Direct and indirect interactions between cannabinoid CB1 receptor and group II metabotropic glutamate receptor signaling in layer V pyramidal neurons from the rat prefrontal cortex. European Journal of Neuroscience, 17(5), 981-990.

Baddeley, A. D. (2002). Is working memory still working?. European psychologist, 7(2), 85.

Barch, D. M., Sheline, Y. I., Csernansky, J. G., & Snyder, A. Z. (2003). Working memory and prefrontal cortex dysfunction: specificity to schizophrenia compared with major depression. Biological psychiatry, 53(5), 376-384.

Baune, B. T., Miller, R., McAfoose, J., Johnson, M., Quirk, F., & Mitchell, D. (2010). The role of cognitive impairment in general functioning in major depression. Psychiatry research, 176(2-3), 183-189.

Bechara, A., Damasio, H., Tranel, D., & Anderson, S. W. (1998). Dissociation of working memory from decision making within the human prefrontal cortex. Journal of neuroscience, 18(1), 428-437.

Bespalov, A., Jongen-Rêlo, A. L., van Gaalen, M., Harich, S., Schoemaker, H., & Gross, G. (2007). Habituation deficits induced by metabotropic glutamate receptors 2/3 receptor blockade in mice: reversal by antipsychotic drugs. Journal of Pharmacology and Experimental Therapeutics, 320(2), 944-950.

Bespalov, A. Y., van Gaalen, M. M., Sukhotina, I. A., Wicke, K., Mezler, M., Schoemaker, H., & Gross, G. (2008). Behavioral characterization of the mGlu

group II/III receptor antagonist, LY-341495, in animal models of anxiety and depression. European journal of pharmacology, 592(1-3), 96-102.

Caraci, F., Nicoletti, F., & Copani, A. (2018). Metabotropic glutamate receptors: the potential for therapeutic applications in Alzheimer's disease. Current opinion in pharmacology, 38, 1- 7.

Cartmell, J., & Schoepp, D. D. (2000). Regulation of neurotransmitter release by metabotropic glutamate receptors. Journal of neurochemistry, 75(3), 889-907.

Chaki, S., Ago, Y., Palucha-Paniewiera, A., Matrisciano, F., & Pilc, A. (2013). mGlu2/3 and mGlu5 receptors: potential targets for novel antidepressants. Neuropharmacology, 66, 40- 52.

Chiriţă, A. L., Gheorman, V., Bondari, D., & Rogoveanu, I. (2015). Current understanding of the neurobiology of major depressive disorder. Rom J Morphol Embryol, 56(2 Suppl), 651-8.

Collingridge, G. L., Peineau, S., Howland, J. G., & Wang, Y. T. (2010). Long-term depression in the CNS. Nature reviews neuroscience, 11(7), 459-473.

Davies, D. A., Greba, Q., & Howland, J. G. (2013). GluN2B-containing NMDA receptors and AMPA receptors in medial prefrontal cortex are necessary for odor span in rats. Frontiers in behavioral neuroscience, 7, 183.

Davies, D. A., Greba, Q., Selk, J. C., Catton, J. K., Baillie, L. D., Mulligan, S. J., & Howland, J. G. (2017). Interactions between medial prefrontal cortex and

dorsomedial striatum are necessary for odor span capacity in rats: role of GluN2B-containing NMDA receptors. Learning & Memory, 24(10), 524-531.

Davies, D. A., Molder, J. J., Greba, Q., & Howland, J. G. (2013). Inactivation of medial prefrontal cortex or acute stress impairs odor span in rats. Learning & Memory, 20(12), 665-669.

Diamond, A. (2013). Executive functions. Annual review of psychology, 64, 135-168.

Doumazane, E., Scholler, P., Zwier, J. M., Trinquet, E., Rondard, P., & Pin, J. P. (2011). A new approach to analyze cell surface protein complexes reveals specific heterodimeric metabotropic glutamate receptors. The FASEB Journal, 25(1), 66-77.

Dudchenko, P. A., Wood, E. R., & Eichenbaum, H. (2000). Neurotoxic hippocampal lesions have no effect on odor span and little effect on odor recognition memory but produce significant impairments on spatial span, recognition, and alternation. Journal of Neuroscience, 20(8), 2964-2977.

Dudchenko, P. A. (2004). An overview of the tasks used to test working memory in rodents. Neuroscience & Biobehavioral Reviews, 28(7), 699-709.

Dutar, P., Vu, H. M., & Perkel, D. J. (1999). Pharmacological characterization of an unusual mGluR-evoked neuronal hyperpolarization mediated by activation of GIRK channels. Neuropharmacology, 38(4), 467-475.

Fava, M., Ball, S., Nelson, J. C., Sparks, J., Konechnik, T., Classi, P., ... & Thase, M. E. (2014). Clinical relevance of fatigue as a residual symptom in major depressive disorder. Depression and anxiety, 31(3), 250-257.

Feyissa, A. M., Woolverton, W. L., Miguel-Hidalgo, J. J., Wang, Z., Kyle, P. B., Hasler, G., ... & Karolewicz, B. (2010). Elevated level of metabotropic glutamate receptor 2/3 in the prefrontal cortex in major depression. Progress in Neuro-Psychopharmacology and Biological Psychiatry, 34(2), 279-283

Ghose, S., Crook, J. M., Bartus, C. L., Sherman, T. G., Herman, M. M., Hyde, T. M., ... & Akil, M. (2008). Metabotropic glutamate receptor 2 and 3 gene expression in the human prefrontal cortex and mesencephalon in schizophrenia. International Journal of Neuroscience, 118(11), 1609-1627.

Granon, S., Vidal, C., Thinus-Blanc, C., Changeux, J. P., & Poucet, B. (1994). Working memory, response selection, and effortful processing in rats with medial prefrontal lesions. Behavioral neuroscience, 108(5), 883.

Gregory, M. L., Stech, N. E., Owens, R. W., & Kalivas, P. W. (2003). Prefrontal group II metabotropic glutamate receptor activation decreases performance on a working memory task. Annals of the New York Academy of Sciences, 1003(1), 405-409.

Gu, G., Lorrain, D. S., Wei, H., Cole, R. L., Zhang, X., Daggett, L. P., ... & Lechner, S. M. (2008). Distribution of metabotropic glutamate 2 and 3 receptors in the rat forebrain: Implication in emotional responses and central disinhibition. Brain research, 1197, 47-62.

Hare, B. D., & Duman, R. S. (2020). Prefrontal cortex circuits in depression and anxiety: contribution of discrete neuronal populations and target regions. Molecular Psychiatry, 1-17.

Harrison, P. J., Lyon, L., Sartorius, L. J., Burnet, P. W. J., & Lane, T. A. (2008). The group II metabotropic glutamate receptor 3 (mGluR3, mGlu3, GRM3): expression, function and Involvement in schizophrenia. Journal of psychopharmacology, 22(3), 308-322.

Higgins, G. A., Ballard, T. M., Kew, J. N., Richards, J. G., Kemp, J. A., Adam, G., ... & Mutel, V. (2004). Pharmacological manipulation of mGlu2 receptors influences cognitive performance in the rodent. Neuropharmacology, 46(7), 907-917.

Iacovelli, L., Nicoletti, F., & De Blasi, A. (2013). Molecular mechanisms that desensitize metabotropic glutamate receptor signaling: an overview. Neuropharmacology, 66, 24-30.

Jaeger, J., Berns, S., Uzelac, S., & Davis-Conway, S. (2006). Neurocognitive deficits and disability in major depressive disorder. Psychiatry research, 145(1), 39-48.

Jazbec, S., McClure, E., Hardin, M., Pine, D. S., & Ernst, M. (2005). Cognitive control under contingencies in anxious and depressed adolescents: an antisaccade task. Biological Psychiatry, 58(8), 632-639.

Johnson, M. P., & Schoepp, D. D. (2008). Group II metabotropic glutamate receptors (mGlu2 and mGlu3). In The Glutamate Receptors (pp. 465-488). Humana Press.

Johnson, B. G., Wright, R. A., Arnold, M. B., Wheeler, W. J., Ornstein, P. L., & Schoepp, D. D. (1999). [3H]-LY341495 as a novel antagonist radioligand for group II metabotropic glutamate (mGlu) receptors: characterization of binding to membranes of mGlu receptor subtype expressing cells. Neuropharmacology, 38(10), 1519-1529.

Kahn, L., Alonso, G., Robbe, D., Bockaert, J., & Manzoni, O. J. (2001). Group 2 metabotropic glutamate receptors induced long term depression in mouse striatal slices. Neuroscience letters, 316(3), 178-182.

Karimi, S. A., Komaki, A., Salehi, I., Sarihi, A., & Shahidi, S. (2015). Role of group II metabotropic glutamate receptors (mGluR2/3) blockade on long-term potentiation in the dentate gyrus region of hippocampus in rats fed with high-fat diet. Neurochemical research, 40(4), 811-817.

Kemp, N., & Bashir, Z. I. (1999). Induction of LTD in the adult hippocampus by the synaptic activation of AMPA/kainate and metabotropic glutamate receptors. Neuropharmacology, 38(4), 495-504.

Kilbride, J., Huang, L., Rowan, M. J., & Anwyl, R. (1998). Presynaptic inhibitory action of the group II metabotropic glutamate receptor agonists, LY354740 and DCG-IV. European journal of pharmacology, 356(2-3), 149-157.

Kiosses, D. N., & Alexopoulos, G. S. (2005). IADL functions, cognitive deficits, and severity of depression: a preliminary study. The American Journal of Geriatric Psychiatry, 13(3), 244-249.

Liu, D., Gu, X., Zhu, J., Zhang, X., Han, Z., Yan, W., ... & Chen, Z. (2014). Medial prefrontal activity during delay period contributes to learning of a working memory task. Science, 346(6208), 458-463.

Liu, J., Zhang, Z., Moreno-Delgado, D., Dalton, J. A., Rovira, X., Trapero, A., ... & Rondard, P. (2017). Allosteric control of an asymmetric transduction in a G protein-coupled receptor heterodimer. Elife, 6, e26985.

Lovinger, D. M., & McCOOL, B. A. (1995). Metabotropic glutamate receptor-mediated presynaptic depression at corticostriatal synapses involves mGLuR2 or 3. Journal of neurophysiology, 73(3), 1076-1083.

Lucas, S. J., Bortolotto, Z. A., Collingridge, G. L., & Lodge, D. (2013). Selective activation of either mGlu2 or mGlu3 receptors can induce LTD in the amygdala. Neuropharmacology, 66, 196-201.

Marazziti, D., Consoli, G., Picchetti, M., Carlini, M., & Faravelli, L. (2010). Cognitive impairment in major depression. European journal of pharmacology, 626(1), 83-86.

Marek, G. J. (2010). Metabotropic glutamate2/3 (mGlu2/3) receptors, schizophrenia and cognition. European journal of pharmacology, 639(1-3), 81-90.

Matsuo, K., Glahn, D. C., Peluso, M. A. M., Hatch, J. P., Monkul, E. S., Najt, P., ... & Fox, P. T. (2007). Prefrontal hyperactivation during working memory task in untreated individuals with major depressive disorder. Molecular psychiatry, 12(2), 158.

Mayberg, H. S., Lozano, A. M., Voon, V., McNeely, H. E., Seminowicz, D., Hamani, C., ... & Kennedy, S. H. (2005). Deep brain stimulation for treatment-resistant depression. Neuron, 45(5), 651-660.

McCall, W. V., & Dunn, A. G. (2003). Cognitive deficits are associated with functional impairment in severely depressed patients. Psychiatry research, 121(2), 179-184.

McIntyre, R. S., Cha, D. S., Soczynska, J. K., Woldeyohannes, H. O., Gallaugher, L. A., Kudlow, P., ... & Baskaran, A. (2013). Cognitive deficits and functional outcomes in major depressive disorder: determinants, substrates, and treatment interventions. Depression and anxiety, 30(6), 515-527.

McIntyre, R. S., Xiao, H. X., Syeda, K., Vinberg, M., Carvalho, A. F., Mansur, R. B., ... & Cha, D. S. (2015). The prevalence, measurement, and treatment of the cognitive dimension/domain in major depressive disorder. CNS drugs, 29(7), 577-589.

McNeely, H. E., Mayberg, H. S., Lozano, A. M., & Kennedy, S. H. (2008). Neuropsychological impact of Cg25 deep brain stimulation for treatment-resistant depression: preliminary results over 12 months. The Journal of nervous and mental disease, 196(5), 405-410.

Müller, N. G., & Knight, R. T. (2006). The functional neuroanatomy of working memory: contributions of human brain lesion studies. Neuroscience, 139(1), 51-58.

Mueller, T. I., Leon, A. C., Keller, M. B., Solomon, D. A., Endicott, J., Coryell, W., ... & Maser, J. D. (1999). Recurrence after recovery from major depressive disorder

during 15 years of observational follow-up. American Journal of Psychiatry, 156(7), 1000-1006.

Mumby, D. G. (2001). Perspectives on object-recognition memory following hippocampal damage: lessons from studies in rats. Behavioural brain research, 127(1-2), 159-181.

National Research Council. (2010). Guide for the care and use of laboratory animals. National Academies Press.

Neki, A., Ohishi, H., Kaneko, T., Shigemoto, R., Nakanishi, S., & Mizuno, N. (1996). Pre-and postsynaptic localization of a metabotropic glutamate receptor, mGluR2, in the rat brain: an immunohistochemical study with a monoclonal antibody. Neuroscience letters, 202(3), 197-200.

NIMH. (2019, February). Major Depression. Retrieved from https://www.nimh.nih.gov/health/statistics/major-depression.shtml.

Otani, S., Daniel, H., Takita, M., & Crepel, F. (2002). Long-term depression induced by postsynaptic group II metabotropic glutamate receptors linked to phospholipase C and intracellular calcium rises in rat prefrontal cortex. Journal of Neuroscience, 22(9), 3434-3444.

Ottersen, O. P., & Landsend, A. S. (1997). Organization of glutamate receptors at the synapse. European Journal of Neuroscience, 9(11), 2219-2224.

Ohishi, H., Shigemoto, R., Nakanishi, S., & Mizuno, N. (1993). Distribution of the messenger RNA for a metabotropic glutamate receptor, mGluR2, in the central nervous system of the rat. Neuroscience, 53(4), 1009-1018.

Ohishi, H., Shigemoto, R., Nakanishi, S., & Mizuno, N. (1993). Distribution of the mRNA for a metabotropic glutamate receptor (mGluR3) in the rat brain: an in situ hybridization study. Journal of Comparative Neurology, 335(2), 252-266.

Papakostas, G. I., Petersen, T., Mahal, Y., Mischoulon, D., Nierenberg, A. A., & Fava, M. (2004). Quality of life assessments in major depressive disorder: a review of the literature. General hospital psychiatry, 26(1), 13-17.

Pehrson, A. L., Jeyarajah, T., & Sanchez, C. (2016). Regional distribution of serotonergic receptors: a systems neuroscience perspective on the downstream effects of the multimodal-acting antidepressant vortioxetine on excitatory and inhibitory neurotransmission. CNS spectrums, 21(2), 162-183.

Petralia, R. S., Wang, Y. X., Niedzielski, A. S., & Wenthold, R. J. (1996). The metabotropic glutamate receptors, mGluR2 and mGluR3, show unique postsynaptic, presynaptic and glial localizations. Neuroscience, 71(4), 949-976.

Pitsikas, N., Kaffe, E., & Markou, A. (2012). The metabotropic glutamate 2/3 receptor antagonist LY341495 differentially affects recognition memory in rats. Behavioural brain research, 230(2), 374-379.

Porter, R. J., Gallagher, P., Thompson, J. M., & Young, A. H. (2003). Neurocognitive impairment in drug-free patients with major depressive disorder. The British Journal of Psychiatry, 182(3), 214-220.

Pu, S., Yamada, T., Yokoyama, K., Matsumura, H., Kobayashi, H., Sasaki, N., ... & Nakagome, K. (2011). A multi-channel near-infrared spectroscopy study of prefrontal cortex activation during working memory task in major depressive disorder. Neuroscience research, 70(1), 91-97.

Rajkowska, G., Miguel-Hidalgo, J. J., Wei, J., Dilley, G., Pittman, S. D., Meltzer, H. Y., ... & Stockmeier, C. A. (1999). Morphometric evidence for neuronal and glial prefrontal cell pathology in major depression. Biological psychiatry, 45(9), 1085-1098.

Richards, G., Messer, J., Malherbe, P., Pink, R., Brockhaus, M., Stadler, H., ... & Mutel, V. (2005). Distribution and abundance of metabotropic glutamate receptor subtype 2 in rat brain revealed by [3H] LY354740 binding in vitro and quantitative radioautography: correlation with the sites of synthesis, expression, and agonist stimulation of [35S] GTPγS binding. Journal of Comparative Neurology, 487(1), 15-27.

Richards, P. M., & Ruff, R. M. (1989). Motivational effects on neuropsychological functioning: comparison of depressed versus nondepressed individuals. Journal of consulting and clinical psychology, 57(3), 396.

Robbe, D., Alonso, G., Chaumont, S., Bockaert, J., & Manzoni, O. J. (2002). Role of p/q-Ca2+ channels in metabotropic glutamate receptor 2/3-dependent presynaptic long-term depression at nucleus accumbens synapses. Journal of Neuroscience, 22(11), 4346-4356.

Roiser, J. P., & Sahakian, B. J. (2013). Hot and cold cognition in depression. CNS spectrums, 18(3), 139-149.

Rose, E. J., & Ebmeier, K. P. (2006). Pattern of impaired working memory during major depression. Journal of affective disorders, 90(2-3), 149-161.

Sanacora, G., Treccani, G., & Popoli, M. (2012). Towards a glutamate hypothesis of depression: an emerging frontier of neuropsychopharmacology for mood disorders. Neuropharmacology, 62(1), 63-77.

Scheurich, A., Fellgiebel, A., Schermuly, I., Bauer, S., Wölfges, R., & Müller, M. J. (2008). Experimental evidence for a motivational origin of cognitive impairment in major depression. Psychological Medicine, 38(2), 237-246.

Schoepp, D. D. (2001). Unveiling the functions of presynaptic metabotropic glutamate receptors in the central nervous system. Journal of Pharmacology and Experimental Therapeutics, 299(1), 12-20.

Schon, K., Tinaz, S., Somers, D. C., & Stern, C. E. (2008). Delayed match to object or place: an event-related fMRI study of short-term stimulus maintenance and the role of stimulus pre-exposure. Neuroimage, 39(2), 857-872.

Shimizu, Y., Kitagawa, N., Mitsui, N., Fujii, Y., Toyomaki, A., Hashimoto, N., ... & Kusumi, I. (2013). Neurocognitive impairments and quality of life in unemployed patients with remitted major depressive disorder. Psychiatry research, 210(3), 913-918.

Spinelli, S., Ballard, T., Gatti-McArthur, S., Richards, G. J., Kapps, M., Woltering, T., ... & Pryce, C. R. (2005). Effects of the mGluR2/3 agonist LY354740 on computerized tasks of attention and working memory in marmoset monkeys. Psychopharmacology, 179(1), 292-302.

Spooren, W., Ballard, T., Gasparini, F., Amalric, M., Mutel, V., & Schreiber, R. (2003). Insight into the function of Group I and Group II metabotropic glutamate (mGlu) receptors: behavioural characterization and implications for the treatment of CNS disorders. Behavioural pharmacology, 14(4), 257-277.

Stern, C. E., Sherman, S. J., Kirchhoff, B. A., & Hasselmo, M. E. (2001). Medial temporal and prefrontal contributions to working memory tasks with novel and familiar stimuli. Hippocampus, 11(4), 337-346.

Suh, Y. H., Chang, K., & Roche, K. W. (2018). Metabotropic glutamate receptor trafficking. Molecular and Cellular Neuroscience, 91, 10-24.

Tanabe, Y., Nomura, A., Masu, M., Shigemoto, R., Mizuno, N., & Nakanishi, S. (1993). Signal transduction, pharmacological properties, and expression patterns of two rat metabotropic glutamate receptors, mGluR3 and mGluR4. Journal of Neuroscience, 13(4), 1372-1378.

R Vose, L., & K Stanton, P. (2017). Synaptic plasticity, metaplasticity and depression. Current neuropharmacology, 15(1), 71-86.

Waterhouse, R. N., Schmidt, M. E., Sultana, A., Schoepp, D. D., Wheeler, W. J., Mozley, P. D., & Laruelle, M. (2003). Evaluation of [3H] LY341495 for labeling group II

metabotropic glutamate receptors in vivo. Nuclear medicine and biology, 30(2), 187-190.

Wierońska, J. M., & Pilc, A. (2009). Metabotropic glutamate receptors in the tripartite synapse as a target for new psychotropic drugs. Neurochemistry international, 55(1-3), 85-97.

Wood, E. R., Dudchenko, P. A., & Eichenbaum, H. (1999). The global record of memory in hippocampal neuronal activity. Nature, 397(6720), 613-616.

Wostrack, M., & Dietrich, D. (2009). Involvement of Group II mGluRs in mossy fiber LTD. Synapse, 63(12), 1060-1068.

World Health Organization (Ed.). (2017, January 3). Depression. Retrieved from https://www.who.int/health-topics/depression#tab=tab_2

Wright, R. A., Arnold, M. B., Wheeler, W. J., Ornstein, P. L., & Schoepp, D. D. (2001). [3H] LY341495 binding to group II metabotropic glutamate receptors in rat brain. Journal of Pharmacology and Experimental Therapeutics, 298(2), 453-460.

Wu, J., Rowan, M. J., & Anwyl, R. (2004). An NMDAR-independent LTP mediated by group II metabotropic glutamate receptors and p42/44 MAP kinase in the dentate gyrus in vitro. Neuropharmacology, 46(3), 311-317.

Xie, X., & Steketee, J. D. (2009). Effects of repeated exposure to cocaine on group II metabotropic glutamate receptor function in the rat medial prefrontal cortex: behavioral and neurochemical studies. Psychopharmacology, 203(3), 501-510.

Yokoi, M., Kobayashi, K., Manabe, T., Takahashi, T., Sakaguchi, I., Katsuura, G., ... & Nakao, K. (1996). Impairment of hippocampal mossy fiber LTD in mice lacking mGluR2. Science, 273(5275), 645-647.

Tables and Figures

Table 1.

Affinity of LY341495 and LY354740 for mGlu Receptors in Rats and Humans

mGlu Group	Receptor	LY341495 Affinity (pKi)		LY354740 Affinity (pKi)	
		Rat	Human	Rat	Human
1	1	ND	7.8	ND	ND
	5	ND	5.1	ND	ND
2	2	7.7-9	8.6	7.8-7.9	6.9
	3	8	8.9	7.3	8.9
3	4	ND	4.7	ND	ND
	6	ND	ND	ND	5.5
	7	ND	6.7	ND	ND
	8	ND	6.8	ND	5.4

Note. Affinities are presented as pKi, or the -log of Ki. Higher values indicate greater affinity. Abbreviations used: ND: Not determined.

Table 2.

List of Spices Used During the DNMS Task

Table of Spices
Fennel seed
Ginger
Parsley
Caraway seed
Oregano
Sage
Anise seed
Mint
Paprika
Jamaican all spice
Thyme
Lemon peel

Table 3.

Raw DNMS Probe Accuracy Data

Rat	Probe	Accuracy
R3	1	1
R5	1	1
R6	1	1
R8	1	1
R9	1	1
R10	1	1
R11	1	1
R14	1	0.83
R16	1	1
R17	1	1
R18	1	0.83
R19	1	1
R21	1	1
R22	1	0.83
R3	2	1
R5	2	1
R6	2	1
R8	2	0.83
R9	2	0.5
R10	2	1
R11	2	0.83
R14	2	0.67
R16	2	0.83
R17	2	0.83
R18	2	0.75
R19	2	1
R21	2	0.67
R22	2	0.83

Table 4.

Raw ITI Accuracy Data

Rat	ITI	Accuracy	Accuracy_Proportion	Group
R3	30	6	1	1
R5	30	6	1	1
R6	30	6	1	1
R8	30	5	0.83	1
R9	30	5	0.83	1
R10	30	6	1	1
R11	30	5	0.83	1
R3	100	4	0.67	1
R5	100	4	0.67	1
R6	100	3	0.5	1
R8	100	5	0.83	1
R9	100	6	1	1
R10	100	3	0.5	1
R11	100	5	0.83	1
R3	300	3	0.5	1
R5	300	1	0.17	1
R6	300	4	0.67	1
R8	300	4	0.67	1
R9	300	3	0.5	1
R10	300	4	0.67	1
R11	300	4	0.67	1
R3	1000	2	0.33	1
R5	1000	2	0.33	1
R6	1000	4	0.67	1
R8	1000	2	0.33	1
R9	1000	4	0.67	1
R10	1000	3	0.5	1
R11	1000	3	0.5	1
R14	300	5	0.83	2
R14	30	3	0.5	2
R14	1000	3	0.5	2
R17	300	4	0.67	2
R14	100	2	0.33	2
R17	1000	4	0.67	2
R17	30	6	1	2
R17	100	4	0.67	2
R18	30	5	0.83	2
R21	1000	4	0.67	2
R18	300	3	0.5	2

R21	300	4	0.67	2
R18	100	4	0.67	2
R21	100	4	0.67	2
R18	1000	3	0.5	2
R21	30	6	1	2

Table 5.

Raw LY341495 Experimental Data

Rat	Group	Drug	Dose	Accuracy	Acc_Percent	Latency	Distance	Speed
5	1	LY341495	0	6	1	4.56	166.45	11.87
3	1	LY341495	0	6	1	5.18	175.59	13.22
11	1	LY341495	0	6	1	5.53	199.89	16.32
6	1	LY341495	0	6	1	4.85	140.56	13.13
18	2	LY341495	0	3	0.5	4.29	210.72	28.47
19	2	LY341495	0	5	0.83	4.52	212.52	27.96
17	2	LY341495	0	6	1	5.96	195.34	23.63
22	2	LY341495	0	5	0.83	9.1	228.04	22.67
6	1	LY341495	0.3	6	1	5.23	202.01	12.72
3	1	LY341495	0.3	5	0.83	5.94	261.55	14.31
11	1	LY341495	0.3	5	0.83	11.65	266.72	11.25
5	1	LY341495	0.3	4	0.67	5.21	218.37	18.4
19	2	LY341495	0.3	6	1	5.54	190.97	23.95
17	2	LY341495	0.3	5	0.83	9.02	231.4	22.55
22	2	LY341495	0.3	2	0.33	6.16	210.67	26.18
18	2	LY341495	0.3	0	0	5.2	188.81	31.85
5	1	LY341495	1	2	0.33	28.14	329.56	9.59
11	1	LY341495	1	6	1	12.63	240.13	11.16
3	1	LY341495	1	5	0.83	11.92	234.65	10.55
6	1	LY341495	1	6	1	9.95	233.41	13.12
17	2	LY341495	1	5	0.83	4.97	214.39	25.79
19	2	LY341495	1	6	1	8.37	216.98	22.15
18	2	LY341495	1	5	0.83	5.9	215.19	23.27
22	2	LY341495	1	6	1	8.34	215.14	26.46
3	1	LY341495	3	2	0.33	3.68	262	22
5	1	LY341495	3	1	0.17	44.48	427.9	8.22
6	1	LY341495	3	5	0.83	10.73	204.72	12.19
11	1	LY341495	3	3	0.5	35.05	431.89	10.42
17	2	LY341495	3	4	0.67	10.44	254.62	20.59
19	2	LY341495	3	5	0.83	14.51	235.08	20.29
22	2	LY341495	3	5	0.83	10.73	235.48	20.96
18	2	LY341495	3	4	0.67	5.93	197.22	29.49

Figure 1.

Model of the mGlu 2/3 Receptors at the Tripartite Synapse

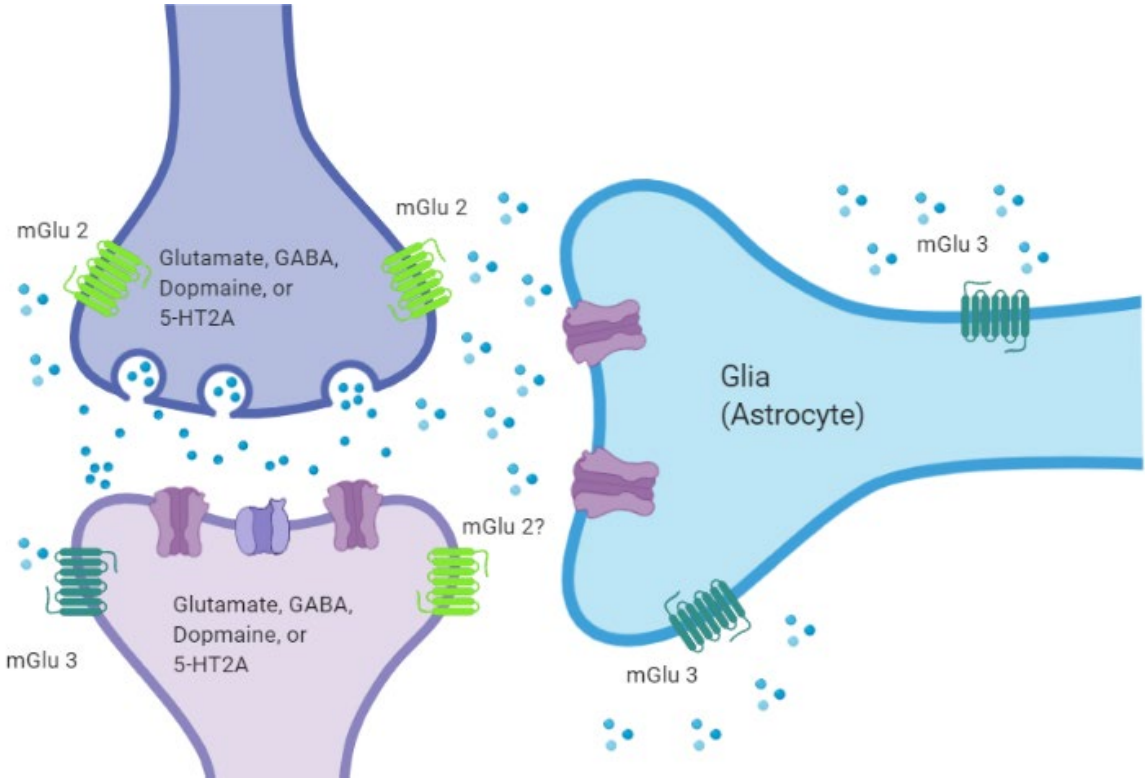

.

Figure 2.

Non-Matching-to-Sample Open Field Designed According to the Specifications of Davies et al. (2004)

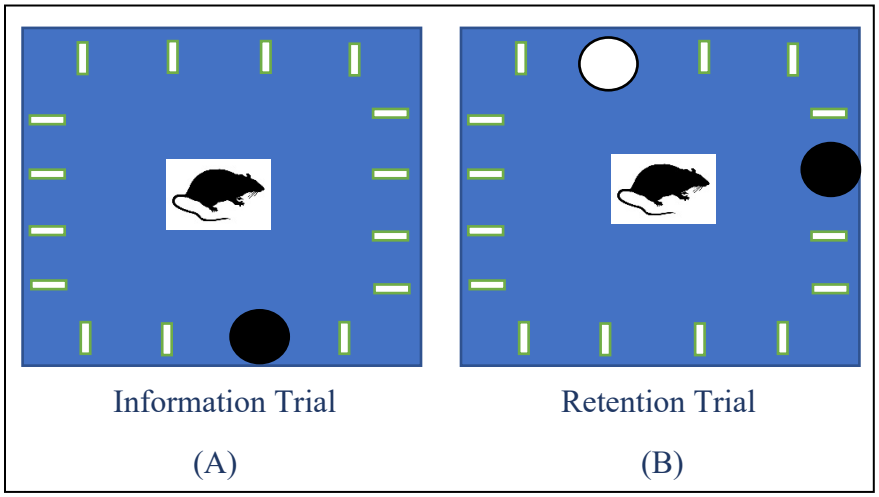

Note. Approximate placing of the scented sand cups during the information (A) and retention trials (B). In the retention trial the old cup (black) was moved to a random location and a novel scented cup (white) was also randomly place on the open field.

Figure 3.

Description of Sample Sizes

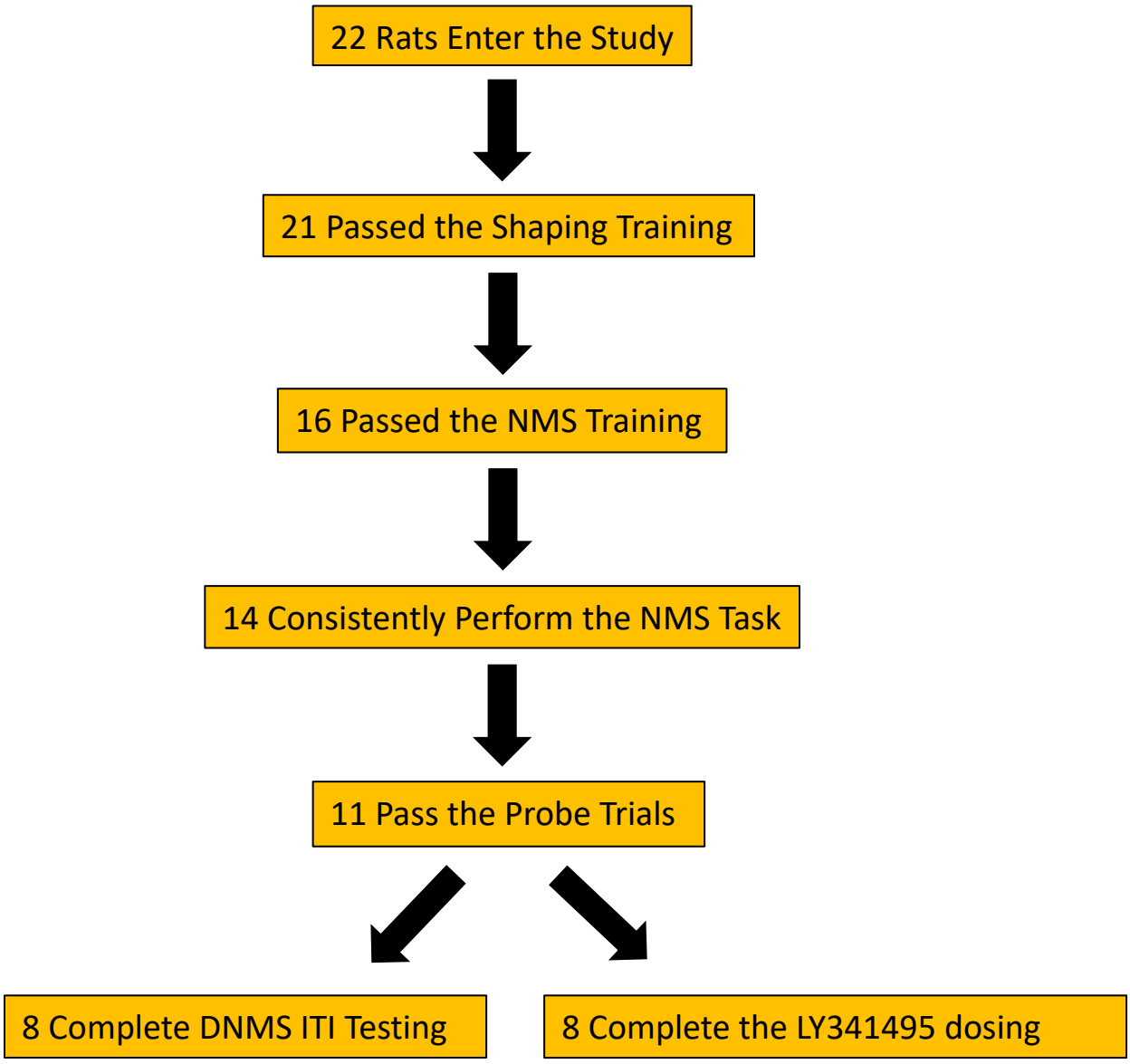

Figure 4.

Training Data

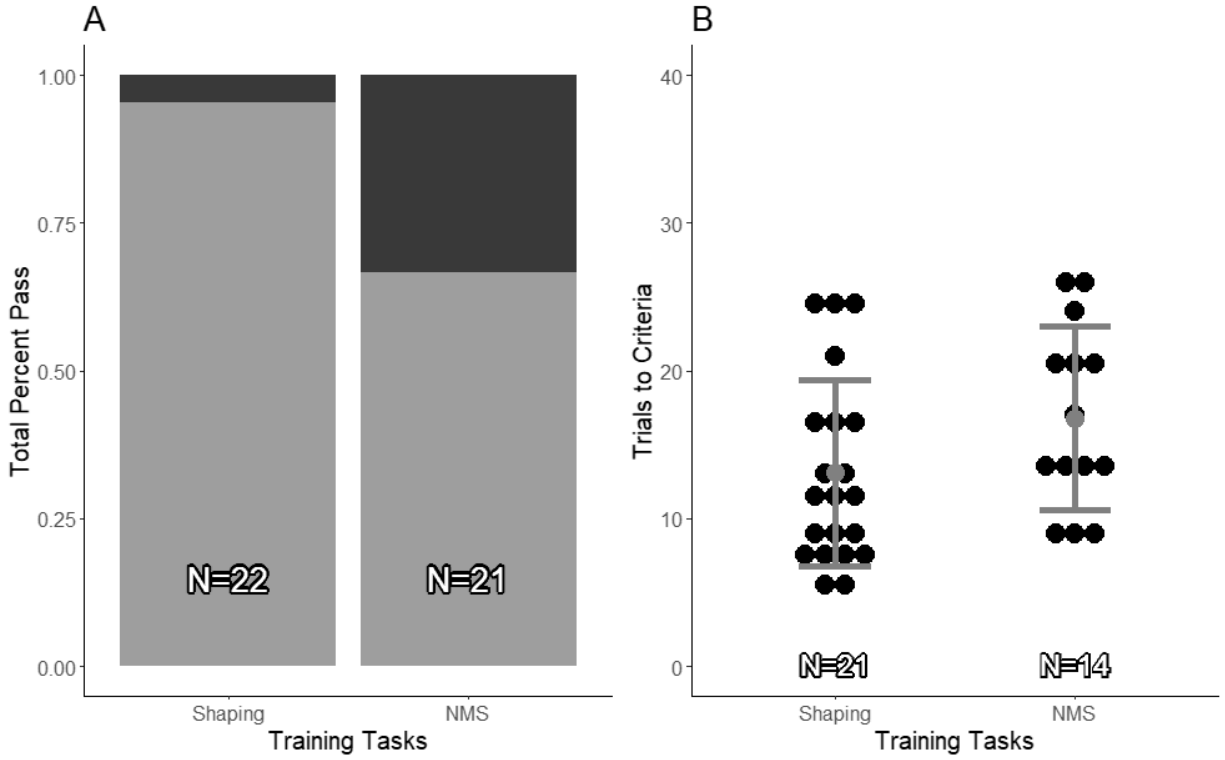

Note. A) Proportion of rats that passed or failed either the shaping (n = 22) or NMS training (n = 21). Yellow represents animals that passed, while purple represents animals that failed. B) Number of trials needed to reach the passing criteria for animals that successfully passed the shaping (n = 21) or NMS task (n = 14). The red bars indicate the mean and ±SEM for the training tasks.

Figure 5.

Accuracy Measures During the DNMS Probe Trials

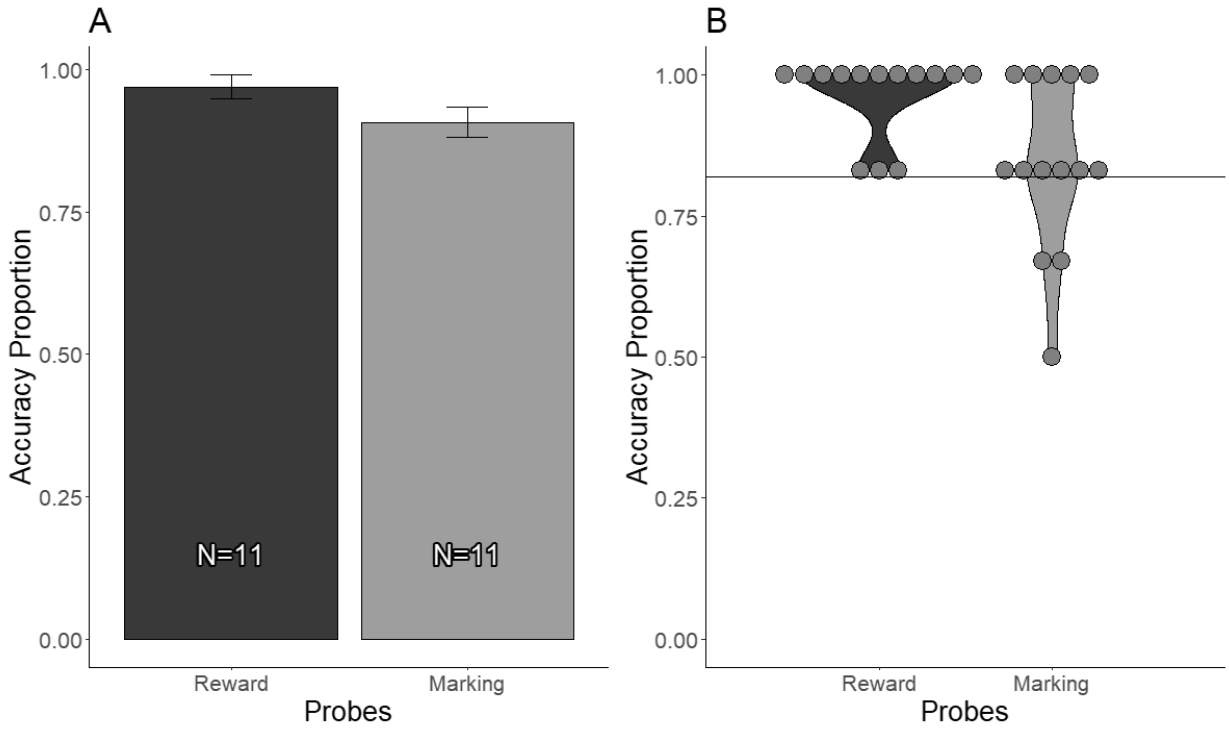

Note. (A) Accuracy scores (±SEM) of the rats who successfully completed both of the probe trials (n = 11). (B) Individual accuracy scores of all rats tested in probe trials (n = 14). The horizontal line represents the passing criterion of 0.833 accuracy or better. All 14 rats passed the reward probe, indicating that the rats were not guided by the scent of the reward. Inspection of the accuracy data during the marking probe revealed that three rats were guided by some form of marking odor, achieving less than < 0.833 accuracy. These animals were removed from any further study. Thus, the animals remaining in the study did not use alternate strategies to perform the DNMS task.

Figure 6.

Accuracy Measures of the ITI on the DMNS Task

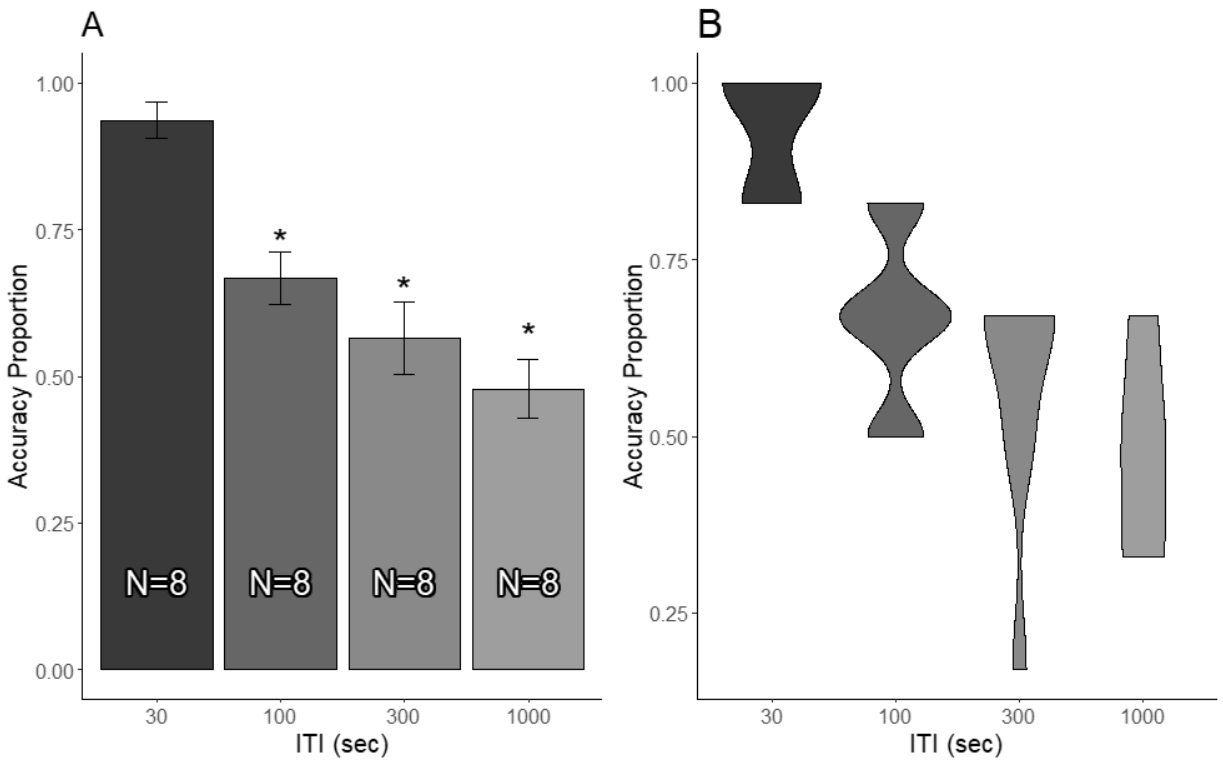

Note. A) DNMS accuracy data after experiencing increasing ITI times expressed as a proportion. There were significant differences in DNMS accuracy between ITIs of 30 seconds and 100 seconds, 30 seconds and 300 seconds, and 30 seconds and 1000 seconds. Data are presented as mean ± SEM. Asterisks represent significant differences from the 30 second ITI (*, $p < 0.05$). B) Violin plots represent the distribution of the individual accuracy scores in response to ITIs.

Figure 7.

LY341495 Treatment Impairs Accuracy in the DNMS Task

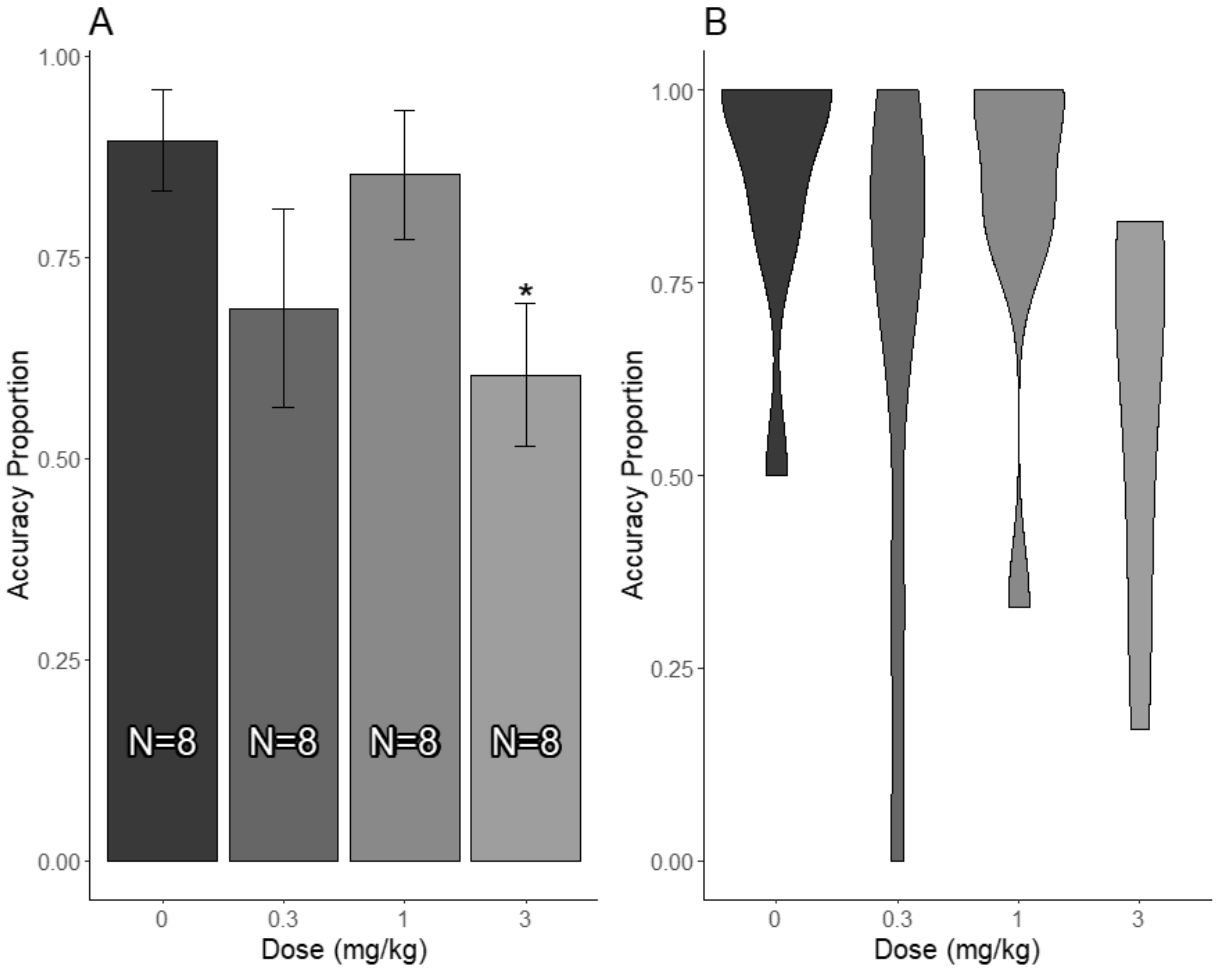

Note. A) DNMS task accuracy data after dosing with LY341495 (0.3, 1 & 3 mg/kg) or vehicle expressed as a proportion. ITI was 100 seconds between the information and retention trials. 3 mg/kg LY341495 30 min IP induced significant impairments in DNMS accuracy compared to vehicle. Data are presented as mean ± SEM. Asterisks represent significant differences from vehicle (*, $p < 0.05$) B) Violin plots represent the distribution of individual accuracy scores in response to LY341495 or vehicle.

Figure 8.

The Effects of LY341495 (30 min IP) Administration on Locomotor Function in the DNMS Task

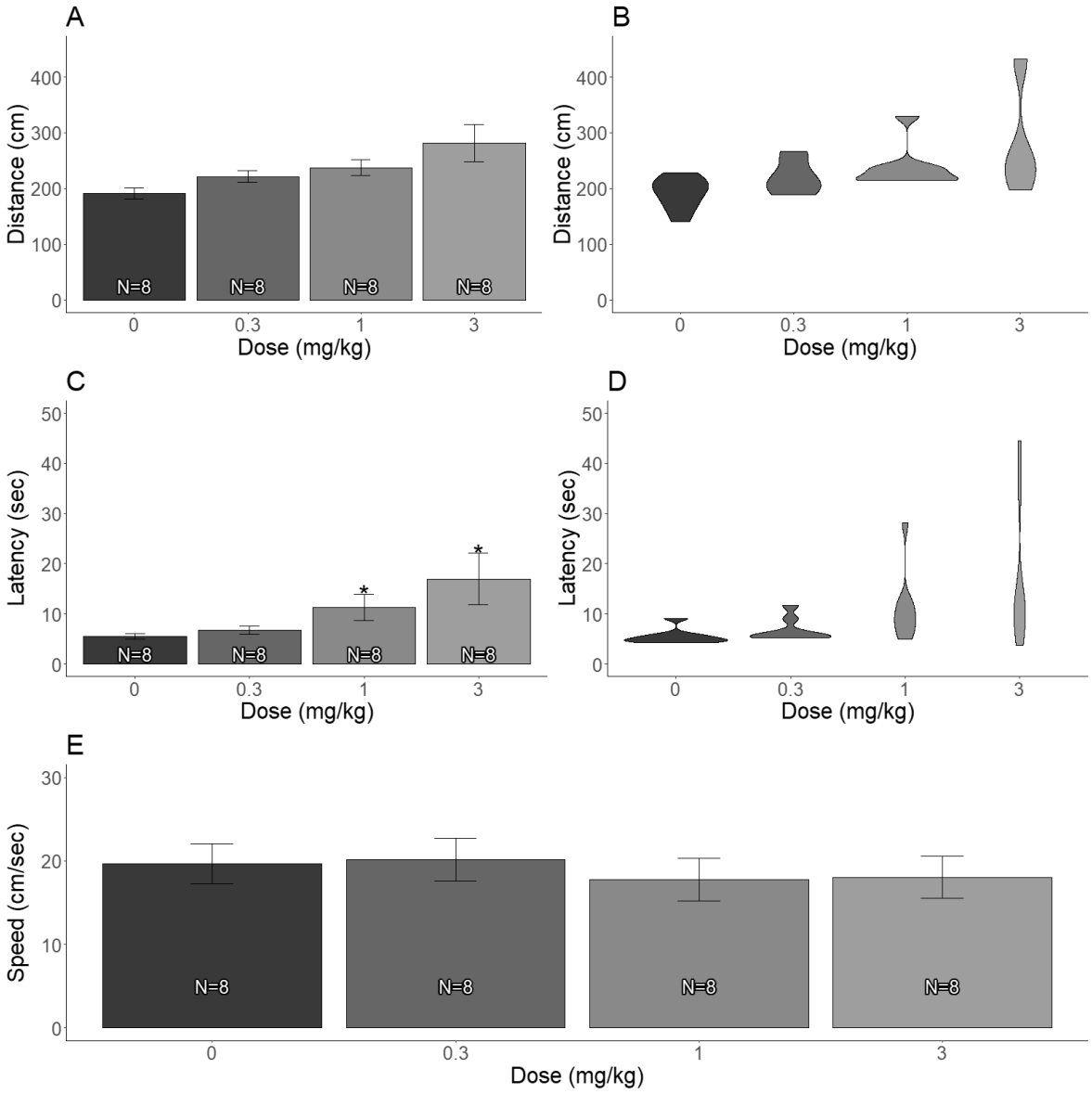

Note. (A, B) LY341495 treatment caused no significant changes compared to vehicle in distance traveled. (C, D) LY341495 treatment significantly increased response latencies at the 1 and 3 mg/kg doses. Data in panels A, C, and E are presented as mean ± SEM. Violin plots represent the pattern of individual distance (Panel B) or latency (Panel D) scores. Asterisks represent significant differences from vehicle (*, $p<0.05$)

Appendix

R Code for the LY341495 Data Analysis

R version 3.6.2 (2019-12-12)

RStudio Version 1.2.5001

```
# Libraries

library(rstudioapi)

setwd(dirname(rstudioapi::getActiveDocumentContext()$path))

library(tidyverse)

library(nortest)

library(rstatix)

library(ez)

library(psychReport)

library(Rmisc)

# Read in the shaping and training data

DNMS_T_S <- read.csv(file='../../Data/DNMS_Training_Shaping_2020317.csv')

# Read Drug Trial csv into R

Drug_Trials <- read_csv(file="../../Data/Drug_Trials/LY341495_CDPPB.csv")

# Read ITI csv into R

ITI_Trials <- read.csv(file= "../../Data/ITI_Trials/ITI.csv")
```

```
# Separates data into seperate Drugs

LY341495 <- Drug_Trials[Drug_Trials$Drug=='LY341495',]

##########################################################################
######

# LY341495 DATA ANALYSIS

#First, data was checked for normality using the Lilliefors test. In cases where data was
distributed normally,

#data was analyzed using a one-way repeated measures ANOVA, with Tukey-Kramer
post hoc tests where appropriate.

#In cases where data was not distributed normally, data was analyzed using Friedman's
test, followed where appropriate

#by the Wilcoxon-Ranked Sign post hoc tests. All data is expressed as mean ± standard
error of the mean (SEM), and

#alpha was set at 0.05.



# Set the doses from numeric to factor

LY341495$Dose <- factor(LY341495$Dose, levels = c('0','0.3','1','3'))

# Filter and group the data by dose

veh <- filter(LY341495, Dose== '0')

D1 <- filter(LY341495, Dose== '0.3')
```

```
D2 <- filter(LY341495, Dose== '1')

D3 <- filter(LY341495, Dose== '3')

##########################################################################
######

# Descriptive stats for shaping and training data

Shaping <- filter(DNMS_T_S, Task==1)

Shaping_Trials_Pass <- filter(Shaping, Pass==1)

Shaping_TTC <-summarySE(Shaping, measurevar = 'Trials_Elapsed', groupvars =
'Task')

Shaping_TTC

Training <- filter(DNMS_T_S, Task==2)

Training_Trials_Pass <- filter(Training, Pass==1)

Training_TTC <-summarySE(Training, measurevar = 'Trials_Elapsed', groupvars =
'Task')

Training_TTC

# Relative Frequency of Passing Training and Shaping

Shaping_Prop <-summarySE(Shaping, measurevar = 'Pass', groupvars = 'Task')

Training_Prop <-summarySE(Training, measurevar = 'Pass', groupvars = 'Task')

DNMS <- rbind(Shaping_Prop,Training_Prop)
```

```
DNMS$Fail <- 1-DNMS$Pass

DNMS_Total_Prop <- DNMS%>%

select(Task,Pass,Fail)#############################################################

######

# Analysis of the Dose data

#############################################################################

######

# Descriptive STATS for the accuracy column

get_summary_stats(LY341495, Accuracy, show = c("mean","sd","se","ci"))

# Calculate the residuals (score - mean(scores))

Aveh_residuals <- tbl_df(veh$Accuracy- mean(veh$Accuracy))

AD1_residuals <- tbl_df(D1$Accuracy- mean(D1$Accuracy))

AD2_residuals <- tbl_df(D1$Accuracy- mean(D2$Accuracy))

AD3_residuals <- tbl_df(D3$Accuracy- mean(D3$Accuracy))

# Put residuals from each dose into a tbl_df

ADose_residuals <- rbind(Aveh_residuals,AD1_residuals,AD2_residuals,AD3_residuals)

# Compute the lilliefors test on those residuals

lillie.test(ADose_residuals$value)

# Run the non-parametric Friedman test ranked sum test
```

```
Acc_FT <- friedman_test(LY341495, Accuracy ~ Dose | Rat)

Acc_FT_EFF <- friedman_effsize(LY341495, Accuracy ~ Dose | Rat)

Acc_FT$EFF <- Acc_FT_EFF$effsize

Acc_FT

# Post hoc test using the Mann-Whitney U (wilcoxon ranked sign) test

Acc_MW <- LY341495 %>% wilcox_test(Accuracy ~ Dose, p.adjust.method = "none",
conf.level = 0.95)

# to calculate the z score use the p value from the wilcox_text divided by 2. Since it is a
2-sided test

Acc_Zstat <- qnorm(Acc_MW$p/2)

# Calculate effect sizes from the wilcox_test

Acc_EFF<- wilcox_effsize(LY341495,Accuracy ~ Dose)

Acc_MW$Z_score <- Acc_Zstat

Acc_MW$Effectsize <- Acc_EFF$effsize

Acc_MW$Magnitude <- Acc_EFF$magnitude

Acc_MW

##########################################################################
######

# Analysis of the distnace data
```

```
##########################################################################
######

# Descriptive STATS for the Distance column

get_summary_stats(LY341495, Distance, show = c("mean","sd","se","ci"))



# Filter and group the data by dose to get the residuals

Dveh_residuals <- tbl_df(veh$Distance- mean(veh$Distance))

DD1_residuals <- tbl_df(D1$Distance- mean(D1$Distance))

DD2_residuals <- tbl_df(D1$Distance- mean(D2$Distance))

DD3_residuals <- tbl_df(D3$Distance- mean(D3$Distance))

# Put residuals from each dose into a tbl_df

DDose_residuals <- rbind(Dveh_residuals,DD1_residuals,DD2_residuals,DD3_residuals)

# Compute the lilliefors test on those residuals

lillie.test(DDose_residuals$value)

# Perform a one-way within-subjects repeated measures ANOVA. DV = Distance, IV =
Dose

# ezANOVA checks the homogeneity of variance using Mauchly's test of Sphericity

Dist_aov <- ezANOVA(LY341495, dv = Distance, wid=Rat, within= Dose, detailed = T,
return_aov = T)
```

```
# Calculate the MSE for the Distance/Dose

Dist_aov$ANOVA$MSE <- Dist_aov$ANOVA$SSd/Dist_aov$ANOVA$DFd

Dist_aov

# Post hoc test to be used is the Tukey-kramer

# Use Alan's manually coded Tukeys.

hsdtukey_stat <- function(group1,group2,MSE,groupno,dferror) {

 n1 <- length(group1)

 n2 <- length(group2)

 mean1 <- mean(group1)

 mean2 <- mean(group2)

 sx = sqrt((MSE/2)*(1/n1 + 1/n2))

 HSD= abs((mean2-mean1)/sx)

 a.05 <- qtukey(0.95,groupno,dferror)

 a.01 <- qtukey(0.99,groupno,dferror)

 a.001 <- qtukey(0.999,groupno,dferror)

 if (HSD>a.001){

  sig<- c('***')

 }else if (HSD>a.01){
```

```
  sig<- c('**')
 }else if (HSD>a.05){
  sig<- c('*')
 }else{
  sig<-c('n.s.')
 }
 tukeylist <- list(HSD, a.05,a.01,a.001, sig)
 return(tukeylist)
}
LY341495_Dose1 <- filter(LY341495, Dose == '0')
LY341495_Dose2<- filter(LY341495, Dose == '0.3')
LY341495_Dose3 <- filter(LY341495, Dose == '1')
LY341495_Dose4 <- filter(LY341495, Dose == '3')
MSE = 2454.475
groupno = 4
dferror = 21
# hsdtukey_stat <- function(group1,group2,MSE,groupno,dferror)
LY341495_tukey_comp1 <- hsdtukey_stat(LY341495_Dose1$Distance,
```

```
                    LY341495_Dose2$Distance,MSE,

                    groupno,dferror)

LY341495_tukey_comp2 <- hsdtukey_stat(LY341495_Dose1$Distance,

                    LY341495_Dose3$Distance,MSE,

                    groupno,dferror)

LY341495_tukey_comp3 <- hsdtukey_stat(LY341495_Dose1$Distance,

                    LY341495_Dose4$Distance,MSE,

                    groupno,dferror)

LY341495_comparisons <- c('Dose1 vs. Dose2','Dose1 vs. Dose3', 'Dose1 vs. Dose4')

LY341495_tukeysig <- c(LY341495_tukey_comp1[5], LY341495_tukey_comp2[5],
LY341495_tukey_comp1[5])

LY341495_posthoc_tbl <- cbind(LY341495_comparisons, LY341495_tukeysig)

LY341495_posthoc_tbl

#########################################################################
######

# Analysis of the Latency data

#########################################################################
######

# Descriptive STATS for the Latency column
```

```
get_summary_stats(LY341495, Latency, show = c("mean","sd","se","ci"))

# Filter and group the data by dose to get the residuals

Lveh_residuals <- tbl_df(veh$Latency- mean(veh$Latency))

LD1_residuals <- tbl_df(D1$Latency- mean(D1$Latency))

LD2_residuals <- tbl_df(D1$Latency- mean(D2$Latency))

LD3_residuals <- tbl_df(D3$Latency- mean(D3$Latency))

# Put residuals from each dose into a tbl_df

LDose_residuals <- rbind(Lveh_residuals,LD1_residuals,LD2_residuals,LD3_residuals)

# Compute the lilliefors test on those residuals

lillie.test(LDose_residuals$value)

Lat_FT <- friedman_test(LY341495, Latency ~ Dose | Rat)

Lat_FT_EFF <- friedman_effsize(LY341495, Latency ~ Dose | Rat)

Lat_FT$EFF <- Lat_FT_EFF$effsize

Lat_FT

Lat_WT <- LY341495 %>% wilcox_test(Latency ~ Dose, p.adjust.method = "none",
conf.level = 0.95)

# Calculate the z scores for the wilcox_test

Lat_Zstat <- qnorm(Lat_WT$p/2)

# Calculate effect sizes from the wilcox_test
```

```
Lat_EFF<- wilcox_effsize(LY341495,Latency ~ Dose)

Lat_WT$Z_score <- Lat_Zstat

Lat_WT$Effectsize <- Lat_EFF$effsize

Lat_WT$Magnitude <- Lat_EFF$magnitude

Lat_WT

################################################################################
######

# Analysis of Speed data

################################################################################
######

# Descriptive STATS for the Speed column

get_summary_stats(LY341495, Speed, show = c("mean","sd","se","ci"))

# Filter and group the data by dose to get the residuals

Sveh_residuals <- tbl_df(veh$Speed- mean(veh$Speed))

SD1_residuals <- tbl_df(D1$Speed- mean(D1$Speed))

SD2_residuals <- tbl_df(D1$Speed- mean(D2$Speed))

SD3_residuals <- tbl_df(D3$Speed- mean(D3$Speed))

# Put residuals from each dose into a tbl_df

SDose_residuals <- rbind(Sveh_residuals,SD1_residuals,SD2_residuals,SD3_residuals)
```

```
# Compute the lilliefors test on those residuals

lillie.test(SDose_residuals$value)

# Compute a one-way repeated measures ANOVA

Speed_aov <- ezANOVA(LY341495, Speed, Rat, Dose, detailed = T, return_aov = T)

Speed_aov

##########################################################################
#####

# Analysis of the ITI Data

##########################################################################
######

ITI_Trials$ITI <- factor(ITI_Trials$ITI, levels = c('30','100','300','1000'))

# Filter and group the data by dose

ITI_1 <- filter(ITI_Trials, ITI== '30')

ITI_2 <- filter(ITI_Trials, ITI== '100')

ITI_3 <- filter(ITI_Trials, ITI== '300')

ITI_4 <- filter(ITI_Trials, ITI== '1000')

# Summary of the ITI data

get_summary_stats(ITI_Trials, Accuracy, show = c("mean","sd","se","ci"))

# Arrange the residuals and group them together
```

```
ITI_1_residuals <- tbl_df(ITI_1$Accuracy- mean(ITI_1$Accuracy))

ITI_2_residuals <- tbl_df(ITI_2$Accuracy- mean(ITI_2$Accuracy))

ITI_3_residuals <- tbl_df(ITI_3$Accuracy- mean(ITI_3$Accuracy))

ITI_4_residuals <- tbl_df(ITI_4$Accuracy- mean(ITI_4$Accuracy))

# Put residuals from each dose into a tbl_df

ITI_residuals <- rbind(ITI_1_residuals,ITI_2_residuals,ITI_3_residuals,ITI_4_residuals)

# Analyze the data for normality using the Lilliefors's test

lillie.test(ITI_residuals$value)

# Run the non-parametric Friedman's test and calculate effect size measures

ITI_FT <- friedman_test(ITI_Trials, Accuracy ~ ITI | Rat)

ITI_FT_EFF <- friedman_effsize(ITI_Trials, Accuracy ~ ITI | Rat)

ITI_FT$EFF <- ITI_FT_EFF$effsize

ITI_FT



# Post hoc test using the Wilcoxon ranked sign test

ITI_WT <- ITI_Trials %>% wilcox_test(Accuracy ~ ITI, p.adjust.method = "none",
conf.level = 0.95)

# To calculate the z score use the p value from the wilcox_text divided by 2. Since it is a
2-sided test
```

```
ITI_Zstat <- qnorm(ITI_WT$p/2)

# Calculate effect sizes from the wilcox_test

ITI_EFF<- wilcox_effsize(ITI_Trials,Accuracy ~ ITI)

# Combine the values into a single table

ITI_WT$Z_score <- ITI_Zstat

ITI_WT$Effectsize <- ITI_EFF$effsize

ITI_WT$Magnitude <- ITI_EFF$magnitude

ITI_WT
```

R Code for the LY341495 Data Visualizations

```
# Libraries

library(rstudioapi)

setwd(dirname(rstudioapi::getActiveDocumentContext()$path))

library(tidyverse)

library(sciplot)

library(Rmisc)

library(patchwork)

library(shadowtext)

library(Hmisc)

################################################################################

####

# Filter Data

# Read CSV into R

#Shaping_Trials_To_Criteria <-

read_csv(file="../../Data/Shaping/Shaping_Trials_To_Criteria.csv")

#Trials_To_Criteria <- read_csv(file="../../Data/Training/Trials_To_Criteria.csv")

Drug_Trials <- read_csv(file="../../Data/Drug_Trials/LY341495_CDPPB.csv")

ITI_Trials <- read.csv(file= "../../Data/ITI_Trials/ITI.csv")
```

```
Probe_trials <- read.csv(file="../../Data/Probes/Probe.csv")

DNMS_T_S <- read.csv(file='../../Data/DNMS_Training_Shaping_2020317.csv')

# Separates data into seperate Drugs

LY341495 <- Drug_Trials[Drug_Trials$Drug=='LY341495',]

# Set the doses from numerics to factors

LY341495$Dose <- factor(LY341495$Dose, levels = c('0','0.3','1','3'))

# Set the ITIs from numerics to factors

ITI_Trials$ITI <- factor(ITI_Trials$ITI, levels = c('30','100','300','1000'))

# Set the Probes from numerics to factors 1 = Reward Probe, 2 = Odor Probe

Probe_trials$Probe <- factor(Probe_trials$Probe, levels = c('1','2'))

# Set the rats as factors for the training and shaping data

DNMS_T_S$Rat <- factor(DNMS_T_S$Rat, levels =

c('1','2','3','4','5','6','7','8','9','10','11','12','13','14','15','16','17','18','19','20','21','22'))

##########################################################################

######

# Accuracy Data Visuals

LY341495_ACC_sum <- summarySE(LY341495, measurevar = 'Acc_Percent',

groupvars = c('Dose'))

LY341495_ACC_sum
```

```
ACC_bar <- ggplot(LY341495_ACC_sum, aes(Dose,Acc_Percent, fill= Dose))+
        geom_bar(stat = 'identity', colour='black')+
        geom_errorbar(aes(ymin=Acc_Percent-se, ymax=Acc_Percent+se),
width=.175)+
        geom_shadowtext(label='N=8', color= 'white', y= 0.15, size= 7)+
        theme_classic()+
        theme(legend.position = 'none', axis.title = element_text(size = 15), axis.text =
element_text(size = 12))+
        labs(y= 'Accuracy Proportion', x= 'Dose (mg/kg)') +
        scale_fill_viridis_d(begin = 0.2, end = 0.9, direction = 1, option = "inferno",
aesthetics = "fill")+
        ggtitle("A")+
        theme(plot.title = element_text(size = 20))


ACC_bar <- ACC_bar + annotate('text', x=4, y=0.7, label = '*', size= 8)
ACC_bar
ACC_violin <- ggplot(LY341495,aes(Dose,Acc_Percent, fill= Dose))+
            geom_violin(colour='black')+
```

```
        theme_classic()+

        scale_fill_viridis_d(begin = 0.2, end = 0.9, direction = 1, option = "inferno",
aesthetics = "fill")+

        ggtitle("B")+

        labs(y= 'Accuracy Proportion', x= 'Dose (mg/kg)') +

        theme(legend.position = 'none', axis.title = element_text(size = 15), axis.text
= element_text(size = 12))+

        theme(plot.title = element_text(size = 20))

ACC_violin

##########################################################################
######

# Distance Data Visuals

LY341495_Dist_sum <- summarySE(LY341495, measurevar = 'Distance', groupvars =
c('Dose'))

LY341495_Dist_sum


Dist_bar <- ggplot(LY341495_Dist_sum, aes(Dose,Distance, fill= Dose))+

    geom_bar(stat = 'identity',colour='black')+

    geom_errorbar(aes(ymin=Distance-se, ymax=Distance+se), width=.175)+
```

```
        geom_shadowtext(label='N=8', color= 'white', y= 25, size= 7)+

        ylim(0,450)+

        theme_classic()+

        scale_fill_viridis_d(begin = 0.2, end = 0.9, direction = 1, option = "inferno",
aesthetics = "fill")+

        ggtitle("A")+

        labs(y= 'Distance (cm)', x= 'Dose (mg/kg)') +

        theme(legend.position = 'none', axis.title = element_text(size = 25), axis.text =
element_text(size = 20))+

        theme(plot.title = element_text(size = 30))
Dist_bar



Dist_violin <- ggplot(LY341495, aes(Dose,Distance, fill= Dose))+

            geom_violin(colour='black')+

            ylim(0,450)+

            theme_classic()+

            scale_fill_viridis_d(begin = 0.2, end = 0.9, direction = 1, option = "inferno",
aesthetics = "fill")+

            ggtitle("B")+
```

```
        labs(y= 'Distance (cm)', x= 'Dose (mg/kg)') +

        theme(legend.position = 'none', axis.title = element_text(size = 25), axis.text
= element_text(size = 20))+

        theme(plot.title = element_text(size = 30))

Dist_violin

##############################################################################
######

# Latency Data Visuals

LY341495_Lat_sum <- summarySE(LY341495, measurevar = 'Latency', groupvars =
c('Dose'))

LY341495_Lat_sum


Lat_bar <- ggplot(LY341495_Lat_sum, aes(Dose,Latency, fill= Dose))+

        geom_bar(stat = 'identity',colour='black')+

        geom_errorbar(aes(ymin=Latency-se, ymax=Latency+se), width=.175)+

        geom_shadowtext(label='N=8', color= 'white', y= 2, size= 7)+

        theme_classic()+

        scale_fill_viridis_d(begin = 0.2, end = 0.9, direction = 1, option = "inferno",
aesthetics = "fill")+
```

```
        ggtitle("C")+
        labs(y= 'Latency (sec)', x= 'Dose (mg/kg)') +
        theme(legend.position = 'none', axis.title = element_text(size = 25), axis.text =
element_text(size = 20))+
        theme(plot.title = element_text(size = 30)) + ylim(0, 50)

Lat_bar <- Lat_bar + annotate('text', x=3, y=14, label = '*', size= 10)+
         annotate('text', x=4, y=22.1, label = '*', size= 10)
Lat_bar

Lat_violin <- ggplot(LY341495, aes(Dose,Latency, fill= Dose))+
        geom_violin(colour='black')+
        theme_classic()+
        scale_fill_viridis_d(begin = 0.2, end = 0.9,direction = 1, option = "inferno",
aesthetics = "fill")+
        ggtitle("D")+
        labs(y= 'Latency (sec)', x= 'Dose (mg/kg)') +
        theme(legend.position = 'none', axis.title = element_text(size = 25), axis.text
= element_text(size = 20))+
```

```
        theme(plot.title = element_text(size = 30)) + ylim(0,50)


Lat_violin

##############################################################################
######

# Speed Data Visuals


############################

LY341495_Sp_sum <- summarySE(LY341495, measurevar = 'Speed', groupvars =
c('Dose'))

LY341495_Sp_sum


Sp_bar <- ggplot(LY341495_Sp_sum, aes(Dose,Speed, fill= Dose))+

        geom_bar(stat = 'identity',colour='black')+

        geom_errorbar(aes(ymin=Speed-se, ymax=Speed+se), width=.175)+

        geom_shadowtext(label='N=8', color= 'white', y= 5,size= 7)+

        theme_classic()+ scale_fill_viridis_d(begin = 0.2, end = 0.9,direction = 1, option
= "inferno", aesthetics = "fill")+

        ggtitle("E")+
```

```
        labs(y= 'Speed (cm/sec)', x= 'Dose (mg/kg)') +

        theme(legend.position = 'none', axis.title = element_text(size = 25), axis.text =
element_text(size = 20))+

        theme(plot.title = element_text(size = 30)) + ylim(0,30)

Sp_bar



Sp_violin <- ggplot(LY341495, aes(Dose,Speed, fill= Dose))+

                geom_violin(colour='black')+

                theme_classic()+

                ggtitle("F")+

                labs(y= 'Speed (cm/sec)', x= 'Dose (mg/kg)') +

                theme(legend.position = 'none')+

                scale_fill_viridis_d(begin = 0.2, end = 0.9,direction = 1, option = "inferno",
aesthetics = "fill")+

                theme(legend.position = 'none', axis.title = element_text(size = 25), axis.text
= element_text(size = 20))+

                theme(plot.title = element_text(size = 30)) + ylim(0,40)



Sp_violin
```

```
##########################################################################
######

# ITI Trials Visuals


ITI_Trials_sum <- summarySE(ITI_Trials, measurevar = 'Accuracy_Proportion',
groupvars = c('ITI'))

ITI_Trials_sum


ITI_bar <- ggplot(ITI_Trials_sum, aes(ITI,Accuracy_Proportion, fill= ITI))+

        geom_bar(stat = 'identity',colour='black')+

        geom_errorbar(aes(ymin=Accuracy_Proportion-se,
ymax=Accuracy_Proportion+se), width=.175)+

        geom_shadowtext(label='N=8', color= 'white', y= 0.15, size= 7)+

        theme_classic()+ scale_fill_viridis_d(begin = 0.2, end = 0.9,direction = 1,
option = "inferno", aesthetics = "fill")+

        ggtitle("A")+

        labs(y= 'Accuracy Proportion', x= 'ITI (sec)') +

        theme(legend.position = 'none', axis.title = element_text(size = 15), axis.text =
element_text(size = 12))+
```

```
        theme(plot.title = element_text(size = 20)) + ylim(0,1)


ITI_bar <- ITI_bar + annotate('text', x=2, y=0.73, label = '*', size= 8)+
          annotate('text', x=3, y=0.65, label = '*', size= 8)+
          annotate('text', x=4, y=0.57, label = '*', size= 8)
ITI_bar


ITI_violin <- ggplot(ITI_Trials, aes(ITI,Accuracy_Proportion, fill= ITI))+
          geom_violin(colour='black')+
          theme_classic()+
          ggtitle("B")+
          labs(y= 'Accuracy Proportion', x= 'ITI (sec)') +
          theme(legend.position = 'none')+
          scale_fill_viridis_d(begin = 0.2, end = 0.9,direction = 1, option = "inferno",
aesthetics = "fill")+
          theme(legend.position = 'none', axis.title = element_text(size = 15), axis.text
= element_text(size = 12))+
          theme(plot.title = element_text(size = 24))
```

```
ITI_violin

##########################################################################
######

# Probe Trial Visuals

# Filter the probe data to remove failures

RewardProbes <- filter(Probe_trials, Probe==1)

OdorProbes <- filter(Probe_trials, Probe==2)



Probes_All <- bind_cols(RewardProbes,OdorProbes)%>%

              select(Rat,Accuracy,Accuracy1)%>%

              mutate(Reward_Acc=Accuracy)%>%

              mutate(Odor_Acc=Accuracy1)%>%

              select(Rat,Reward_Acc,Odor_Acc)



PP <- filter(Probes_All, Reward_Acc>=0.83 & Odor_Acc>=0.83)

RP <- PP%>% select(Rat, Reward_Acc)%>%

      mutate(Accuracy=Reward_Acc)%>%

      mutate(Probe=rep(1,times=length(Rat)))%>%

      select(Rat,Probe,Accuracy)
```

```
OP <- PP%>% select(Rat, Odor_Acc)%>%
        mutate(Accuracy=Odor_Acc)%>%
        mutate(Probe=rep(2,times=length(Rat)))%>%
        select(Rat,Probe,Accuracy)

PT_Passes <- bind_rows(RP,OP)
PT_Passes$Probe <- factor(PT_Passes$Probe, levels = c('1','2'))

Probe_Trial_sum<- summarySE(PT_Passes, measurevar = "Accuracy", groupvars =
'Probe')
Probe_Trial_sum

Probe_Trial_Bar <- ggplot(Probe_Trial_sum, aes(Probe,Accuracy, fill=Probe))+
            geom_bar(stat='identity', colour='black')+
            geom_errorbar(aes(ymin=Accuracy-se, ymax=Accuracy+se), width=.175)+
            geom_shadowtext(label='N=10', color= 'white', y= 0.15, size= 7)+
            theme_classic()+
```

```
        theme(legend.position = 'none', axis.title = element_text(size = 20), axis.text
= element_text(size = 16))+

        labs(y= 'Accuracy Proportion', x= 'Probes') +

        scale_fill_viridis_d(begin = 0.2, end = 0.9, direction = 1, option = "inferno",
aesthetics = "fill")+

        ggtitle("A")+

        theme(plot.title = element_text(size = 25))



Probe_Trial_Bar<- Probe_Trial_Bar + scale_x_discrete(breaks=c('1','2'),labels=
c('Reward','Marking'))

Probe_Trial_Bar



Probe_Trial_violin <- ggplot(Probe_trials, aes(Probe,Accuracy, fill=Probe))+

          geom_violin(colour='black')+

          theme_classic()+

          ggtitle("B")+

          labs(y= 'Accuracy Proportion', x= 'Probes') +

          theme(legend.position = 'none')+
```

```
                scale_fill_viridis_d(begin = 0.2, end = 0.9,direction = 1, option = "inferno",
aesthetics = "fill")+

                theme(legend.position = 'none', axis.title = element_text(size = 20),
axis.text = element_text(size = 16))+

                theme(plot.title = element_text(size = 25)) + ylim(0,1)+

                scale_x_discrete(breaks=c('1','2'),labels= c('Reward','Marking'))



Probe_Trial_violin <- Probe_Trial_violin + geom_dotplot(binaxis='y', stackdir='center',
dotsize=1, fill='green')

Probe_Trial_violin <- Probe_Trial_violin+ annotate('segment', x=0, xend = 3, y=0.82,
yend = 0.82)

Probe_Trial_violin

################################################################################
######

# Training anad Shaping Trials to Criteria visuals

Shaping <- filter(DNMS_T_S, Task==1)

Shaping_Prop <-summarySE(Shaping, measurevar = 'Pass', groupvars = 'Task')



Training <- filter(DNMS_T_S, Task==2)
```

```
Training_Prop <-summarySE(Training, measurevar = 'Pass', groupvars = 'Task')



DNMS <- rbind(Shaping_Prop,Training_Prop)

DNMS$Fail <- 1-DNMS$Pass

DNMS <- DNMS%>% select(Task,Pass,Fail)



DNMS <-DNMS %>% gather('Pass','Fail',2:3)%>%

        mutate(Pass_Fail=Pass)%>%

        mutate(Rel_Freq=Fail)%>%

        select(Task,Pass_Fail,Rel_Freq)



DNMS$Task <- factor(DNMS$Task, levels = c('1','2'))



DNMS_Training_Bar <- ggplot(DNMS, aes(Task,Rel_Freq, fill= Pass_Fail))+

                geom_bar(position = 'stack', stat='identity')+

                theme_classic()+

                geom_shadowtext(label='N=22', color= 'white', x= 1, y= 0.15, size= 7)+

                geom_shadowtext(label='N=21', color= 'white', x= 2, y= 0.15, size= 7)+
```

```
                theme(legend.position = 'none', axis.title = element_text(size = 15),
axis.text = element_text(size = 12))+

                labs(y= 'Total Percent Pass', x= 'Training Tasks') +

                scale_fill_viridis_d(begin = 0.2, end = 0.9, direction = 1, option =
"inferno", aesthetics = "fill")+

                ggtitle("A")+

                theme(plot.title = element_text(size = 20))+

                scale_x_discrete(breaks=c('1','2'),labels= c('Shaping','NMS'))

DNMS_Training_Bar



#filter these to remove anyone that hasnt passed

DNMS_T_S$Task <- factor(DNMS_T_S$Task, levels = c('1','2'))

DNMS_T_S <- filter(DNMS_T_S, Pass==1)

DNMS_T_S_Sum <- summarySE(DNMS_T_S, measurevar = 'Trials_Elapsed',
groupvars = 'Task')

DNMS_T_S_Sum



DNMS_Training_dotplot <- ggplot(DNMS_T_S, aes(Task,Trials_Elapsed))+

                geom_dotplot(binaxis = 'y', stackdir = 'center')+
```

```
                theme_classic()+

                geom_shadowtext(label='N=22', color= 'white', x= 1, y= 0.15, size= 6)+

                geom_shadowtext(label='N=14', color= 'white', x= 2, y= 0.15, size= 6)+

                theme(legend.position = 'none', axis.title = element_text(size = 15),
axis.text = element_text(size = 12))+

                labs(y= 'Trials to Criteria', x= 'Training Tasks')+ ylim(0,40)+

                scale_fill_viridis_d(begin = 0.2, end = 0.9, direction = 1, option =
"inferno", aesthetics = "fill")+

                ggtitle("B")+

                theme(plot.title = element_text(size = 20))+

                scale_x_discrete(breaks=c('1','2'),labels= c('Shaping','NMS'))



DNMS_Training_dotplot <- DNMS_Training_dotplot
+stat_summary(fun.data=mean_sdl, fun.args = list(mult=1),

                        geom="errorbar", color="red", width=0.3, size=2) +

                        stat_summary(fun.y=mean, geom="point", color="red", size=5)

##########################################################################
######

# My data quilts
```

```
Quilt1 <- ACC_bar + ACC_violin

Quilt1


Quilt2 <- (Dist_bar + Lat_bar)/ (Dist_violin + Lat_violin) / Sp_bar

Quilt2


Quilt3 <- ITI_bar + ITI_violin

Quilt3


Quilt4 <- Probe_Trial_Bar + Probe_Trial_violin

Quilt4


Quilt5 <- DNMS_Training_Bar + DNMS_Training_dotplot

Quilt5
```